

Measurement of the Thickness of Liquid Film by Means of Capacitance Method

NP-1212
Research Project 1379-1

Interim Report, November 1979

Prepared by

LAWRENCE BERKELEY LABORATORY
University of California
#1 Cyclotron Road
Berkeley, California 94720

Principal Investigator
B. Leskovar

Co-Investigators
R. K. Sun
W. F. Kolbe
B. Turko

DISCLAIMER

This book was prepared as an account of work sponsored by an agency of the United States Government. Neither the United States Government nor any agency thereof, nor any of their employees, makes any warranty, express or implied, or assumes any legal liability or responsibility for the accuracy, completeness, or usefulness of any information, apparatus, product, or process disclosed, or represents that its use would not infringe privately owned rights. Reference herein to any specific commercial product, process, or service by trade name, trademark, manufacturer, or otherwise, does not necessarily constitute or imply its endorsement, recommendation, or favoring by the United States Government or any agency thereof. The views and opinions of authors expressed herein do not necessarily state or reflect those of the United States Government or any agency thereof.

Prepared for

Electric Power Research Institute
3412 Hillview Avenue
Palo Alto, California 94304

EPRI Project Manager
J. P. Sursock
Nuclear Power Division

DISCLAIMER

This report was prepared as an account of work sponsored by an agency of the United States Government. Neither the United States Government nor any agency thereof, nor any of their employees, makes any warranty, express or implied, or assumes any legal liability or responsibility for the accuracy, completeness, or usefulness of any information, apparatus, product, or process disclosed, or represents that its use would not infringe privately owned rights. Reference herein to any specific commercial product, process, or service by trade name, trademark, manufacturer, or otherwise does not necessarily constitute or imply its endorsement, recommendation, or favoring by the United States Government or any agency thereof. The views and opinions of authors expressed herein do not necessarily state or reflect those of the United States Government or any agency thereof.

DISCLAIMER

Portions of this document may be illegible in electronic image products. Images are produced from the best available original document.

ORDERING INFORMATION

Requests for copies of this report should be directed to Research Reports Center (RRC), Box 10090, Palo Alto, CA 94303, (415) 961-9043. There is no charge for reports requested by EPRI member utilities and affiliates, contributing nonmembers, U.S. utility associations, U.S. government agencies (federal, state, and local), media, and foreign organizations with which EPRI has an information exchange agreement. On request, RRC will send a catalog of EPRI reports.


EPRI authorizes the reproduction and distribution of all or any portion of this report and the preparation of any derivative work based on this report, in each case on the condition that any such reproduction, distribution, and preparation shall acknowledge this report and EPRI as the source.

NOTICE

This report was prepared by the organization(s) named below as an account of work sponsored by the Electric Power Research Institute, Inc. (EPRI). Neither EPRI, members of EPRI, the organization(s) named below, nor any person acting on their behalf: (a) makes any warranty or representation, express or implied, with respect to the accuracy, completeness, or usefulness of the information contained in this report, or that the use of any information, apparatus, method, or process disclosed in this report may not infringe privately owned rights; or (b) assumes any liabilities with respect to the use of, or for damages resulting from the use of, any information, apparatus, method, or process disclosed in this report.

Prepared by
Lawrence Berkeley Laboratory
Berkeley, California

EPRI PERSPECTIVE

PROJECT DESCRIPTION

Annular two-phase flow is often predicted to occur in postulated light water reactor (LWR) accidents and under normal operation, in the shell side of most modern pressurized water reactor (PWR) steam generators. Thus, thermal-hydraulic codes, related to the operation and safety analysis of LWR components, must incorporate accurate empirical data for adequate modeling of this important type of flow.

This report describes a technique measuring the liquid film thickness in annular flows by means of a capacitance bridge. Although this concept is not new, the reader will find that considerable thought was given to refine the technique and improve accuracy.

The method described herein could be used by physicists and engineers engaged in analysis and observation of subscale structures of two-phase flow regimes. In particular the development of local probes with high frequency response should enable one to measure the shape and frequency of disturbance- and roll-waves on thin liquid films. Having such quantitative information will provide a means for developing and/or validating analytical models that are the basis of sophisticated reactor performance and reactor safety calculations.

PROJECT OBJECTIVES

The work discussed in this report is part of a larger effort to develop optical-electronic instrumentation systems for the measurement of key two-phase flow-parameters such as droplet size, velocity distributions, and entrainment thresholds in annular two-phase flow.

New concepts and techniques are now being developed based on laser illumination and image-analyzing methods. They will be the object of a future report in the second quarter of 1980.

PROJECT RESULTS

After completion of this work, the new instrumentation system is expected to be used in other EPRI projects concerned with the observation and measurement of the small-scale structure of two-phase flows; the ultimate goal is to improve thermal-hydraulic modeling of LWRs.

The present report should therefore be considered only as an interim report. More information regarding this and other topics will be published in the final report.

Jean-Pierre Sursock, Project Manager
Nuclear Power Division

ABSTRACT

A technique has been developed for measuring water film thickness in a two phase annular flow system by means of the capacitance method. Theoretical considerations are applied to estimate the capacitance value as function of the film thickness. An experimental model of the flow system with two types of electrodes mounted on the inner wall of a cylindrical tube has been constructed and evaluated. The ability of the apparatus to observe fluctuations and wave motions of the water film passing over the electrodes is described.

CONTENTS

<u>Section</u>	<u>Page</u>
1 INTRODUCTION	1-1
2 GENERAL CONSIDERATIONS OF CAPACITIVE ELECTRODE MEASURING SYSTEM	2-1
3 DESIGN OF THE APPARATUS FOR ANNULAR FLOW EXPERIMENTS	3-1
Design of the Ring-Type Electrode	3-1
Design of Ring-Type Electrodes	3-3
4 CALIBRATION OF ELECTRODES	4-1
Static Calibration	4-1
Dynamic Calibration	4-3
Instrumentation for Capacitance Measurement	4-5
5 EXPERIMENTAL RESULTS	5-1
Selection of Electrode Patterns for the Rod-Type Electrode Pair	5-1
Comparisons Between Static and Dynamic Measurements	5-2
Influence of Water Temperature and Conductivity on Film Thickness Measurement	5-5
6 DISCUSSIONS AND CONCLUSIONS	6-1
7 APPENDIX A DERIVATION OF EQUATION 2-1	A-1
8 REFERENCE LIST	R-1

ILLUSTRATIONS

<u>Figure</u>		<u>Page</u>
2-1	Comparison of Theoretical Values and Measured Values of Reference (6)	2-3
2-2	Pattern of Different Kinds of Printed Circuit Electrode Pairs	2-4
3-1	Comparison of Printed Circuit Electrodes of Different Patterns	3-2
3-2	Construction of Rod Electrode Mounting Block	3-4
3-3	Rod Electrodes of Different Design	3-5
3-4	Construction of Ring Electrode Mounting Section	3-7
4-1	Equipment Set-up for Static Calibration	4-2
4-2	Assembly of the Dynamic Test Section	4-4
4-3	Water Film Thickness as a Function of Flow Rate	4-6
5-1	Comparison Between Theoretical and Measured Values of a Coaxial Electrode Pair	5-3
5-2	Experimental Results of Calibrations of Rod Electrodes (Static and Dynamic)	5-4
5-3	Static Calibration Curves of a Ring Electrode with LCW and TW	5-6
5-4	Dynamic Calibration of the Ring Electrode	5-7
5-5	Arrangement of an External Capacitance for Improving Q Factor	5-8
6-1	Transient Measurements of Film Thickness With Ring Electrodes	6-3
6-2	Transient Measurements of Film Thickness With Rod Electrodes	6-4
A-1	Simple Conformal Transformation of Coplanar Electrode Pair (Hyperbolic Function)	A-2
A-2	Field Plotting of Coplanar Electrode Pair With Transformation $Z = SnW$ (Elliptical Function)	A-3
A-3	Parallel Electrode Geometry with Two Dielectric Substances in Gap	A-5

TABLES

<u>Table</u>		<u>Page</u>
5-1	Static Measurement of Rod-Type Electrodes With a 6 mm Diameter and 0.8 mm Insulation Gap	5-10
5-2	Dynamic Measurements of Rod Electrodes	5-12
5-3	Static Measurements of Ring Electrodes Using Strips	5-16
5-4	Dynamic Measurements of Ring Electrodes	5-19

SUMMARY

A two phase flow system where the liquid and gaseous phases are confined to the interior of a cylindrical tube can be characterized by an annular film of liquid flowing along the wall and a dispersion of droplets and gaseous components in the center. It is important to measure the thickness of the annular film in order to study the properties of such a system.

Among a number of techniques for measuring film thickness, the most common one is the conductivity method which utilizes conducting probes to monitor the resistance of the fluid film. In the case of pure water, the conductivity is too low to render reliable results. A capacitance method is elected for the present study, based upon the fact that the dielectric constant of pure water is very large (by a factor of about 80) in comparison to that of the surrounding gaseous phase. The capacitive probe in addition is non-intrusive and will not disturb the flow, and the response time of the capacitance meter is short enough to observe wave motions and other fluctuations in the film.

To permit an estimation of the electrode capacitance changes, a theoretical equation is provided for the calculation of the effect of the water layer on the surface. The results are compared with experimental measurements and are in good agreement.

Two kinds of electrodes are investigated. One type in the shape of a rod is useful for small area detection, and the second in the form of a ring is appropriate for obtaining average data around the perimeter of the tube's inside wall. The rod-type electrode is designed to have a simple pattern within a circular area of 6 mm in diameter and to be readily replaced without dismantling the flowing system. The electrode pair is capable of measuring film thickness up to 3 mm. The sensitivity of the device is limited by the size of the probe. The ring electrode pair was constructed to have the same inside diameter as that of the annular tube. The width of the electrode, and the gap between them, are made equal to 0.125",

3.1 mm, for a flow tube of 1 $\frac{1}{4}$ " inside diameter. The sensitivity of the ring electrode is adequate for the measurement of water film thicknesses up to 6 mm.

Calibrations of the electrodes are carried out with static and dynamic methods for both kinds of electrodes. It is found that the results are in very good agreement with each other. In order to minimize the effects of temperature and conductivity changes in the fluid on the measurement, an external capacitance can be employed in parallel with the probe to improve the Q factor of the circuit, thereby improving the performance of the capacitance meter.

The capacitance meter has a fast response time (cutoff frequency = 600 Hz) and is sensitive enough to detect a capacitance change of 0.01 pF in 2 ms. Since the meter is provided with an analog output, it is possible to detect the fluctuations and wave motions of the water film passing over the probes by recording the capacitance changes produced by them in a storage oscilloscope or other recorder. The capacitance probes are non-intrusive and do not require doping or other modification of the water.

Section 1

INTRODUCTION

Some two phase flow systems, in which the liquid and gaseous phases are confined to the interior of a cylindrical tube, are characterized by an annular film of liquid which flows along the wall of the tube, and by an interior dispersion of droplets and gaseous components. In order to study the properties of such systems, it is important to measure with some precision, the thickness of the annular film.

Previous studies have shown that this film may range in thickness from zero or nearly zero, to several millimeters or more, and, in the case of slug flow, may even fill the entire tube. Moreover, the film thickness is known to vary rapidly with time and position due to the presence of waves of various frequencies and forms of turbulent behavior.

A valid thickness measurement technique should satisfy several criteria. Because of the presence of wave motions and other disturbances, it should be capable of rapid response. For similar reasons it should average its measurement over as small an area as possible unless only average data are desired. It should be non-intrusive, i.e. it should not disturb the system being measured. Finally, it should not require that the fluid, in this case water, be unrealistically altered by the addition of seeding materials or ionic salts.

A number of techniques have been employed in the past to make film thickness measurements (1-15). Of these, the most common method (1) has been to exploit the difference in conductivity between the liquid and gaseous phase. Conductivity probes flush mounted in the wall of the tube, sense the resistance of the fluid and hence, the thickness. Penetrating conductivity probes (2,3) in the form of insulated needles with conductive ends have also been employed to estimate the film thickness. Unfortunately, the conductivity of pure water

is so low that these methods have, for the most part, required the addition of ionic salts to make reliable measurements possible.

In the present study, we have elected to use the capacitance method to measure the film thickness. In this method, which was first described by Dukler, et al (4, 5) and further developed by Ozgu and Chen (6), use is made of the fact that the dielectric constant of water is 80 times as large as that of the surrounding gaseous phase. If a capacitor, consisting of two small plates mounted on the interior surface of the tube, is covered by a water film, the capacitance will increase as the film thickness is increased. Once the system is calibrated, the capacitance, and hence the film thickness, can be determined with a commercial capacitance meter. The method has the advantage that, unlike the conductivity technique, it can be made to work reliably with pure water. The response time is limited only by the capabilities of the capacitance meter, and, as will be shown, is short enough to observe wave motions and other fluctuations in the film thickness.

In the next section, a theoretical calculation of the effect of the water layer on the capacitor plates is given. This calculation enables us to predict the approximate performance of various probe geometries in order to determine optimum behavior. In the section following, the design of two types of electrodes suitable for annular flow measurements is described. In section 4 the methods employed for the calibration of the capacitance probes are outlined, and in section 5 the experimental results of the calibration are presented.

Section 2

GENERAL CONSIDERATIONS OF CAPACITIVE ELECTRODE MEASURING SYSTEM

A convenient geometrical arrangement for the capacitance measurement of the film thickness consists of a pair of concentric metallic rings mounted coaxially in the wall of the flow tube. Electrodes of this type have been described elsewhere (6). The dimensions of these electrodes are characterized by the perimeter of the rings, $\ell = \pi D$, where D is the diameter of the tube, the width of the rings, a , and d , their separation. Because such electrodes will average the film thickness measurement around the perimeter of the tube, it is desirable to consider also smaller electrodes capable of measuring the thickness at a point on the tube wall. These electrodes would consist of a pair of small metal plates mounted on the interior surface of the tube. By analogy with the ring electrodes, we can consider these electrodes to have a separation, d , and characteristic dimension, a .

In the case of the ring electrodes, the length, ℓ , is much larger than the width, a . The rings can be unrolled and, for the purposes of an approximate calculation, considered to be parallel, coplanar strips of infinite length. Under this condition the capacitance per unit length, C/ℓ , can be estimated to be (Appendix A)

$$\frac{C}{\ell} = \frac{k\epsilon_0}{\pi} \left[V_1 + \int_{V_1}^{V_3} \frac{dV}{1 + \frac{2(k-1)}{\pi} \cos^{-1} \left(\frac{\sinh V_1}{\sinh V} \right)} \right. \\ \left. - \int_{V_2}^{V_3} \frac{Adv}{1 + \frac{2(k-1)}{\pi} \cos^{-1} \left(\frac{\sinh V_1}{\sinh V} \right)} \right] \quad (2-1)$$

where

k = dielectric constant of the fluid

l = length of electrode

$$V_1 = \operatorname{Sinh}^{-1}\left(\frac{2t}{d}\right) \quad (2-2)$$

$$V_2 = \operatorname{Cosh}^{-1}\left(1 + \frac{2a}{d}\right) \quad (2-3)$$

$$V_3 = \frac{\pi}{8} + \operatorname{Cosh}^{-1}\left(1 + \frac{2a}{d}\right) \quad (2-4)$$

A = a correction factor

= 0 for $V_1 < V_2$

$$= \exp\left[-\frac{8}{\pi}(V_1 - V_2)\right] \text{ for } V_2 < V_1 \quad (2-5)$$

The last term of Eq. 2-1 accounts for both the fringe effect of the electrodes and the saturation which occurs when the water film thickness becomes large.

Equation 2-1 is illustrated in Fig. 2-1 for the case of a pair of parallel strips (corresponding to a pair of ring electrodes) satisfying the condition $a/d = 1$ and covered by a water film thickness, t , of a dielectric constant $k = 80$. In the figure the capacitance is expressed as a percentage of the saturation value and as a function of the ratio t/d .

The small circles on the dotted line in Fig. 2-1 are measured values reported by Ozgu and Chen (6), using two brass strip electrodes of length equal to 80 mm, width 2.38 mm and gap 2.38 mm. The saturation capacitance value was measured to be 37.5pF, while the value calculated from the above equation is 40.28pF. The theoretical formula does not apply to the small electrodes of different cross sectional patterns shown in Fig. 2-2. Such electrodes exhibit fringe effects in all directions which are not possible to include in a simple equation like eq. 2-1. However, an electrode pair of coaxial shape such as shown in Fig. 2-2D, can be considered as the transformation of a pair of ring electrodes, and the theoretical considerations given above are still valid to some extent. An example is given in the following section.

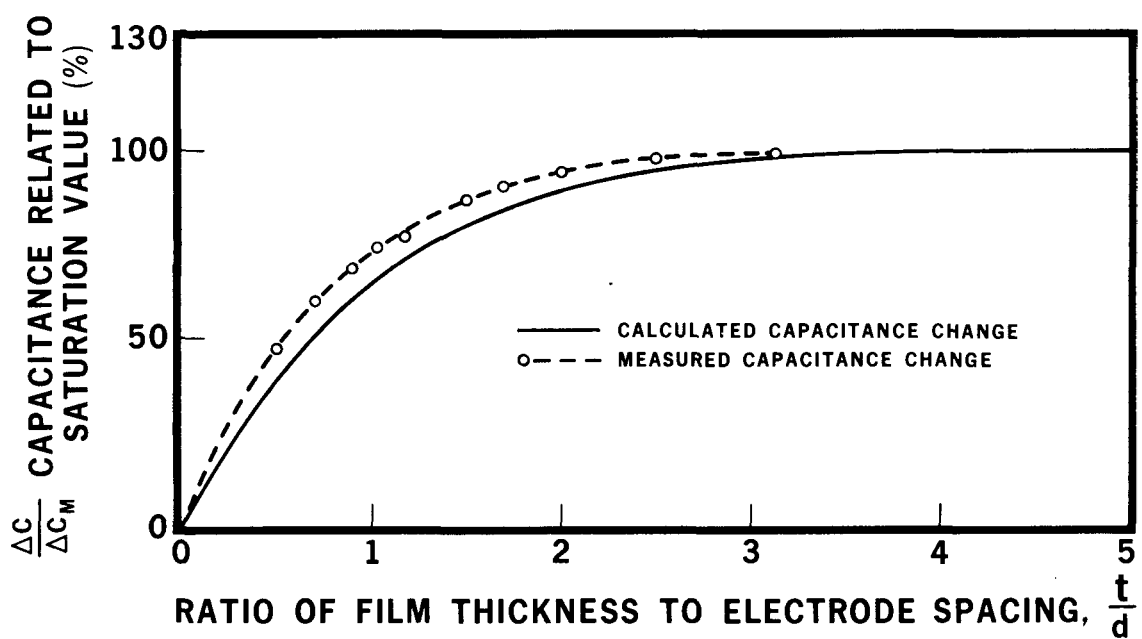


Figure 2-1. Comparison of Theoretical Values and Measured Values of Reference (6)

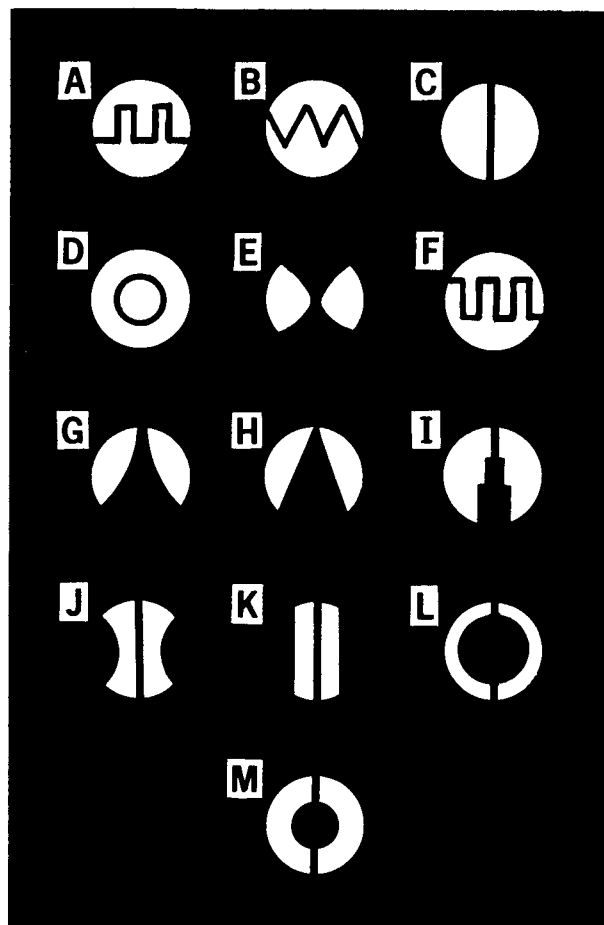


Figure 2-2. Pattern of Different Kinds of Printed Circuit Electrode Pairs

Section 3

DESIGN OF THE APPARATUS FOR ANNULAR FLOW EXPERIMENTS

The design of the experimental apparatus may be divided into two parts, namely the electrodes and the two-phase flow system. It was decided that a plexi-glass tube of $1\frac{1}{4}$ " inside diameter should be used for the experiment, and that electrodes of the rod-type were desirable for the detection of local film thickness, while electrodes of the ring-type were more suitable for monitoring the average film thickness with large dynamic range. The rod-type electrodes are in reality a pair of small electrodes of a given configuration on the end of a cylindrical rod of small diameter (4 to 6 mm). The ends of the electrodes are flush mounted with the inner surface of the flow tube and appear as two small metallic plates separated by an insulation gap.

DESIGN OF ROD-TYPE ELECTRODES

To design electrodes of the rod-type for thickness measurements, there are two factors to be considered, the sensitivity of the electrode and the dynamic range of operation. The former factor is limited by the size of the electrode which should be as small as possible in order to monitor the local film precisely, and the latter is determined by the shape of the electrode pair on the rod.

Electrodes with a narrower gap and larger area will yield a larger capacitance, however, the dynamic range of operation will be increased with the width of the gap because it requires a thicker fluid film to reach saturation with a larger gap. To select a proper shape and size of electrode, different patterns of electrode pairs were made on printed circuit board and tested by covering them with a water film of known thickness. The variety of geometrical sizes and shapes considered is shown in Fig. 2-2. Fig. 3-1 shows the change in capacitance measured in each case as a function of the water film thickness. As a reasonable compromise, the configuration C of Fig. 2-2

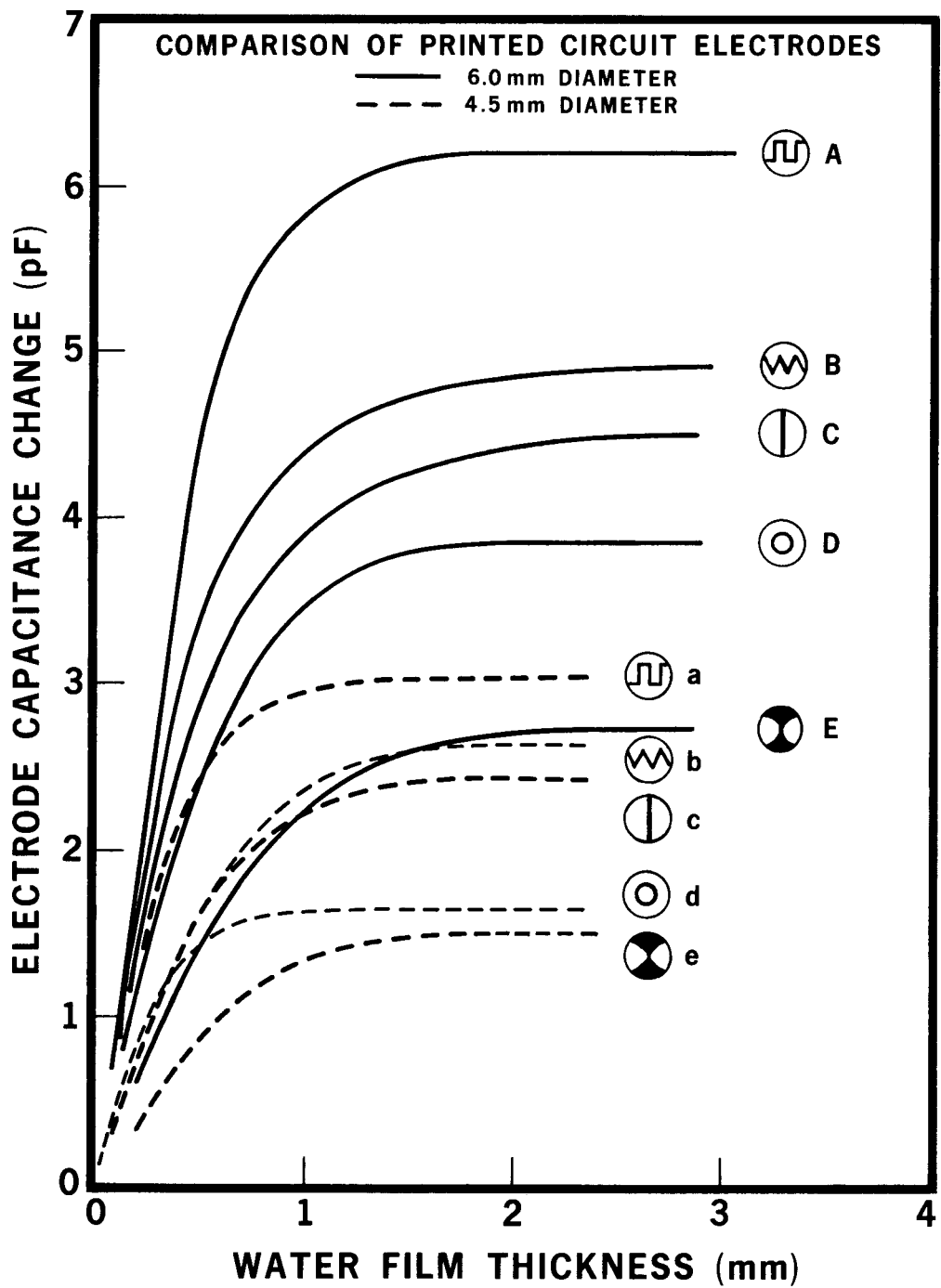


Figure 3-1. Comparison of Printed Circuit Electrodes of Different Patterns

with a diameter of 6 mm and a gap of 0.8 mm along the diameter, was the final selection. This kind of electrode pair can be made of copper plates separated by a thin layer of bakelite of a given thickness. The materials were first glued together to form a single piece and then machined to the right size. An alternative method preparing a rod electrode pair was to use a ceramic rod ground to a cylinder of proper dimensions, then coated with nichrome at high vacuum, having a narrow insulated gap across the diameter at both ends and along the length of the rod. This kind of electrode pair has a low initial capacitance, a high Q, because of its high parallel resistance (in the megohm range) and is suitable for high temperature operation due to the good thermal stability of the substrate material.

The rod electrodes can be constructed independently without considering the size of the annular flow pipe, except that the end of the electrode, which is to be inserted into the flow tube should be machined to the right curvature so that it will be flush with the tube's inner wall. This end of the electrode was coated with a gold layer. The mounting of the rod electrodes in the tube was achieved by means of an attaching block, Fig. 3-2, which was provided with rubber O-rings to stop the leakage of water, with BNC connectors for the output signal, and a shielding metallic box to screen off local interference. Rod electrodes made of rigid coaxial conductors have also been investigated. However, because of their low sensitivity, small dynamic range, and difficulty of construction, they are not recommended for practical application. Samples of the electrodes constructed are illustrated in Fig. 3-3. The rod electrode has the advantage that it can be removed readily without dismantling the flowing system.

DESIGN OF THE RING-TYPE ELECTRODE

The ring electrode pair was constructed to be the same size as the annular tube. It consisted of copper rings embedded in the inner wall of the tube, separated by a gap of the same material as the tube. Both the rings and the gap were designed to have the same width i.e. 1/8" and a diameter of 1 $\frac{1}{4}$ ". The electrode section was an integrated part of the pipe and cannot be changed easily without disturbing the test system. A shielding case was also provided for the ring electrode section to screen off interference. The photo and sketch in Fig. 3-4 shows the construction in detail. The selection of $d = a = \frac{1}{8}$ inch for the ring electrode pair was based on the following

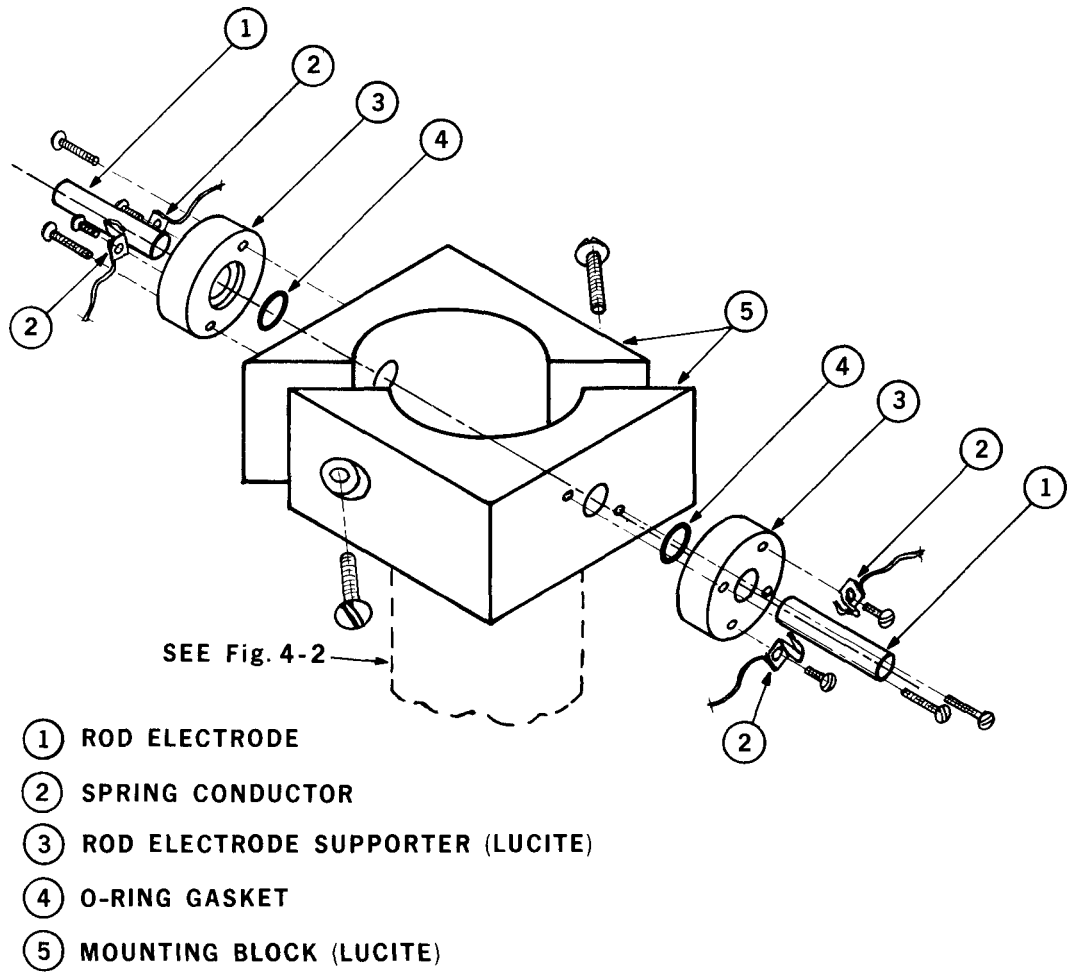


Figure 3-2. Construction of Rod Electrode Mounting Block

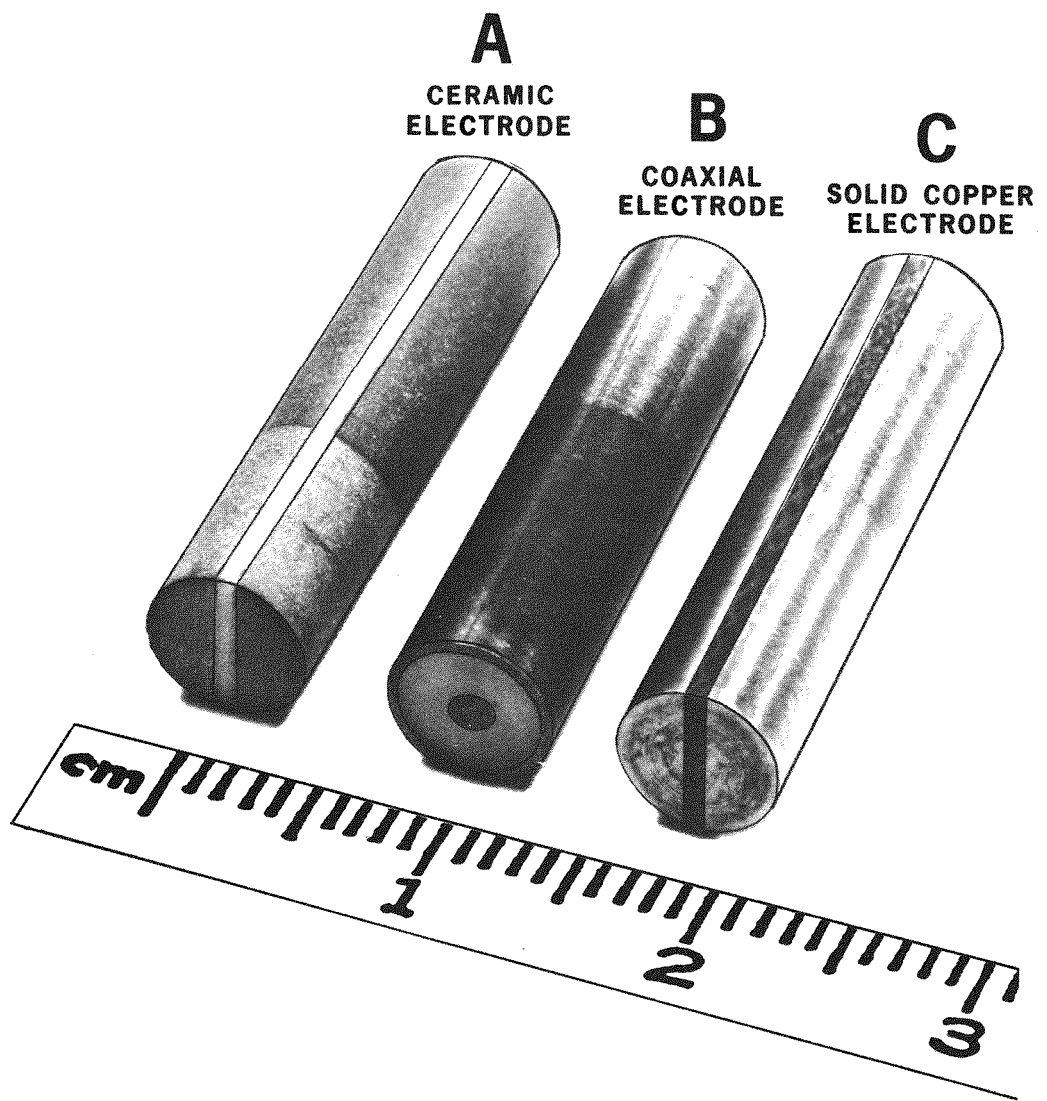


Figure 3-3. Rod Electrodes of Different Design

considerations. According to the theoretical calculation (e.g. Fig. 2-1 solid curve), the change of capacitance is large within the range $0 < \frac{t}{d} < 2$ and saturates at about $\frac{t}{d} = 5$. If the annular tube has an inside diameter of $1\frac{1}{4}'' = 31.75$ mm, the electrode should be able to measure a water thickness up to half of this value, i.e. $t_s = 15.88$ mm. Assuming this for the saturated capacitance, the electrode should have a gap of $d = \frac{t_s}{5} = 3.17$ mm $\approx \frac{1}{8}''$. In order to obtain an accurate measurement at the location under investigation, the ring electrode pair should not have an axial length of more than 10 mm, ($\sim \frac{1}{3}$ of the tube inside diameter). Using $a = d = \frac{1}{8}''$, the total dimension will be $2a + d = \frac{3}{8}'' = 9.53$ mm, which is close to the requirement, and the electrode will have good sensitivity with water film thickness up to $2d = \frac{1}{4}''$ or 6 mm. This is the optimized ring dimension we used.

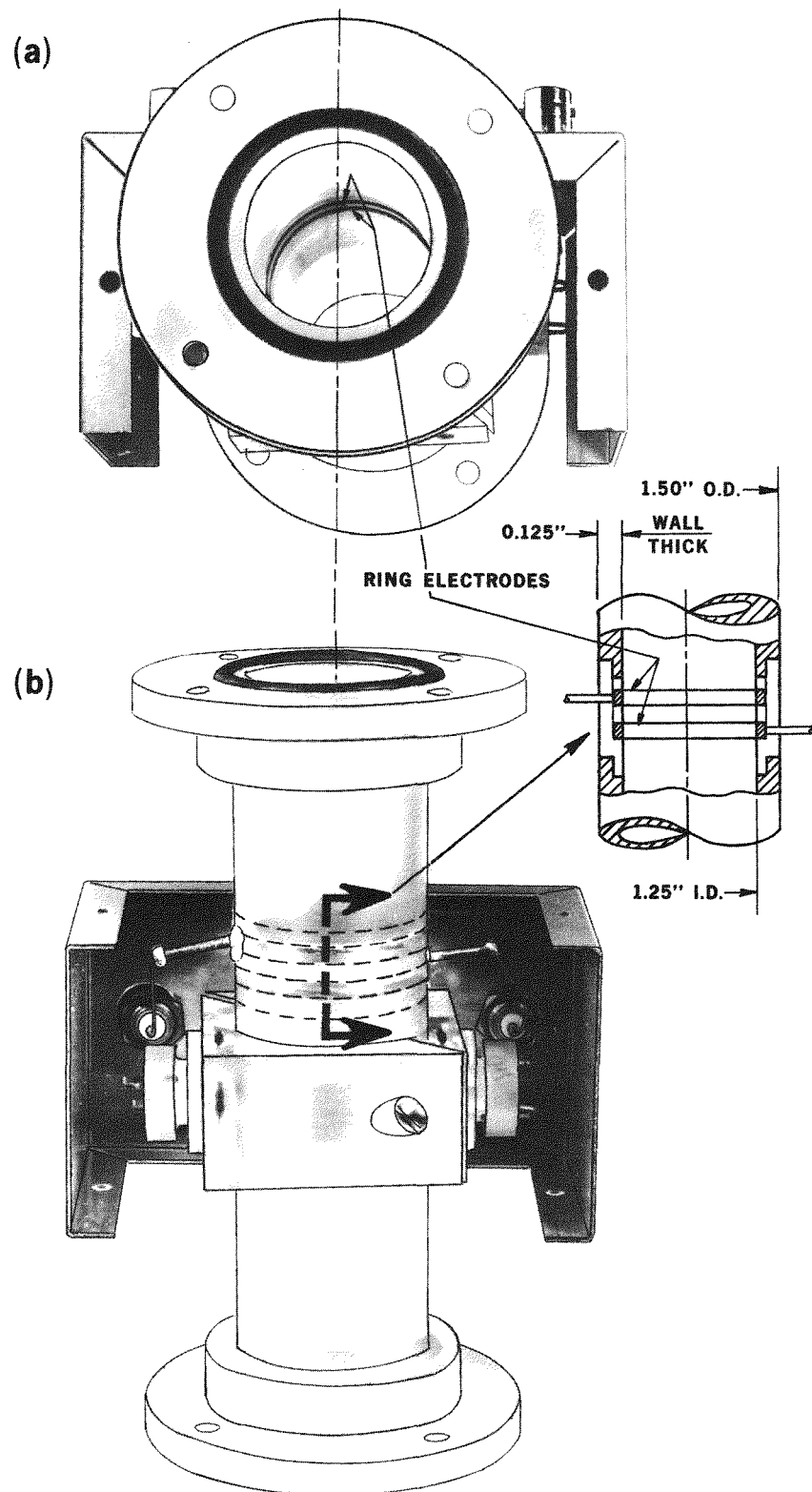


Figure 3-4. Construction of Ring Electrode Mounting Section

Section 4

CALIBRATION OF ELECTRODES

The calibration of the electrodes was implemented by two methods. A static calibration was performed by covering the electrode surface with a stationary film of water of known thickness, and the capacitance value was taken as a function of water film thickness. For the dynamic calibration, a specially constructed flow system was designed. This system consists of a section of pipe into which the electrodes, (rod-type or ring-type) can be mounted. The capacitances of the electrodes were measured with running water of known thickness, flowing along the inner wall of the pipe and over the surface of the electrodes continuously. The water film thickness along the tube's inner wall is a function of the measured flow-rate of the water as explained below.

STATIC CALIBRATION

The apparatus for static calibration consisted of water containers of carefully controlled dimensions. For the rod electrodes a cylindrical water container made of plexiglass was designed having a hole in the bottom so that the rod electrode could be inserted into it, flush with the bottom surface (Fig. 4-1a). The water film thickness on top of the electrode was determined by two independent methods, (1) by calculation from a known volume of fluid in the container and (2) by detection of the water surface with a microscope device which was specially designed to measure thickness down to 0.1μ . Different kinds of water, namely low conductivity water (LCW), tap water (TW), distilled water (DW), and de-ionized water (DIW), were employed for the calibration. The conductivities, δ , of different fluids are as follows:

$$\delta_{LCW} = 6.67 \mu\text{S}/\text{cm}, \delta_{TW} = 66.7 \mu\text{S}/\text{cm}, \delta_{DW} = 2.0 \mu\text{S}/\text{cm}, \text{ and}$$

$$\delta_{DIW} = 2.63 \mu\text{S}/\text{cm}. \text{ Among them the LCW and TW were used most frequently.}$$

For the static calibration of the ring electrodes, a rectangular water tank, with a leveling screw for fine level adjustment, was used (Fig. 4-1b). Copper strips of identical gap width and length as the actual ring electrode pair

(a)

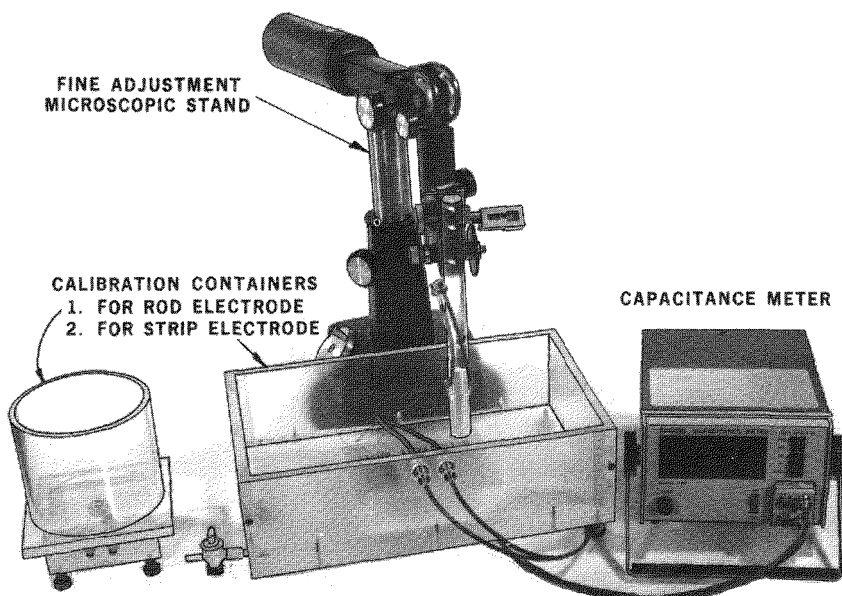
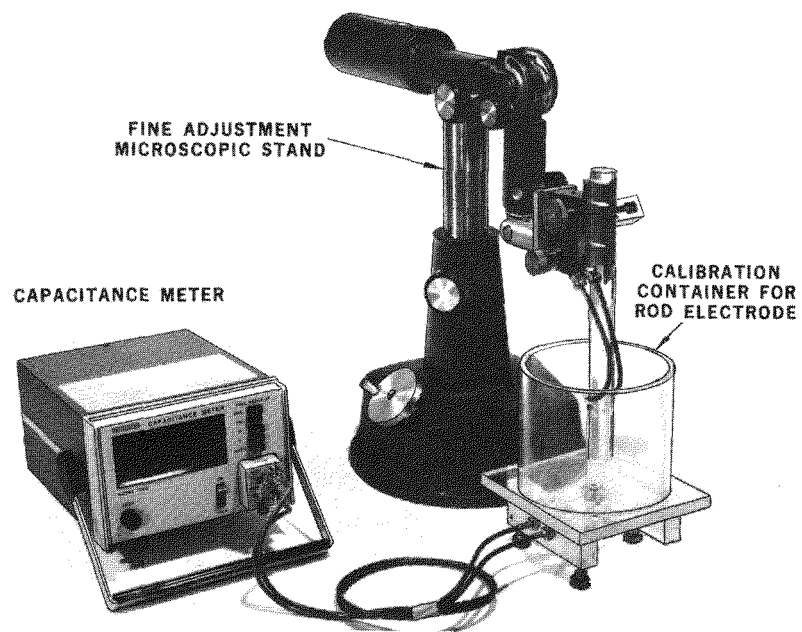


Figure 4-1. Equipment Set-up for Static Calibration

were prepared on a printed circuit board which was adjusted and checked with a water-bubble gauge to make sure that it was parallel to the water surface. Since the electrode's surface was not flush with the bottom of the water tank, the elevation of the electrode's surface and thickness of the first water layer had to be determined by means of a microscope. Thereafter, the measurement of the water thickness was accomplished as described in the last paragraph. The use of copper strips to replace the ring electrodes for static calibration may introduce a discrepancy between the calibration and the true ring electrode value. However, because of the relatively large inner diameter of the tube in comparison to the width and gap length of the electrode, a pair of flat strips were considered to be adequate for the first calibration, as had been previously described elsewhere (6). The tests were done mainly with low conductivity and tap water at room temperature.

DYNAMIC CALIBRATION

The apparatus for the dynamic calibration of the capacitance probes is shown in Fig. 4-2. It consists of a porous plastic water injection tube mounted in a plexiglass water jacket. Attached beneath the injection tube is a length of 1 $\frac{1}{4}$ " ID plexiglass tubing onto which short sections of plexiglass containing the probes are mounted. Water from the supply was passed through calibrated turbine flowmeters (Flow Technology Inc., models FT-12N25-LJC and FTM-N10-LJS) before being introduced to the test apparatus. The flow rate was measured to a precision of better than 1% using a frequency counter and the manufacturer's calibration charts.

The thickness of a falling film of water flowing down the inside of the tube is quoted by Wallis (19). At low flow rates, the film flow is laminar and obeys the equation

$$\delta = \left(\frac{3\mu_f Q_f}{\pi g \rho_f D} \right)^{1/3}$$

where δ is the film thickness. μ_f is the water viscosity, Q_f is the volumetric flow rate, g is the gravitational acceleration, ρ_f is the water

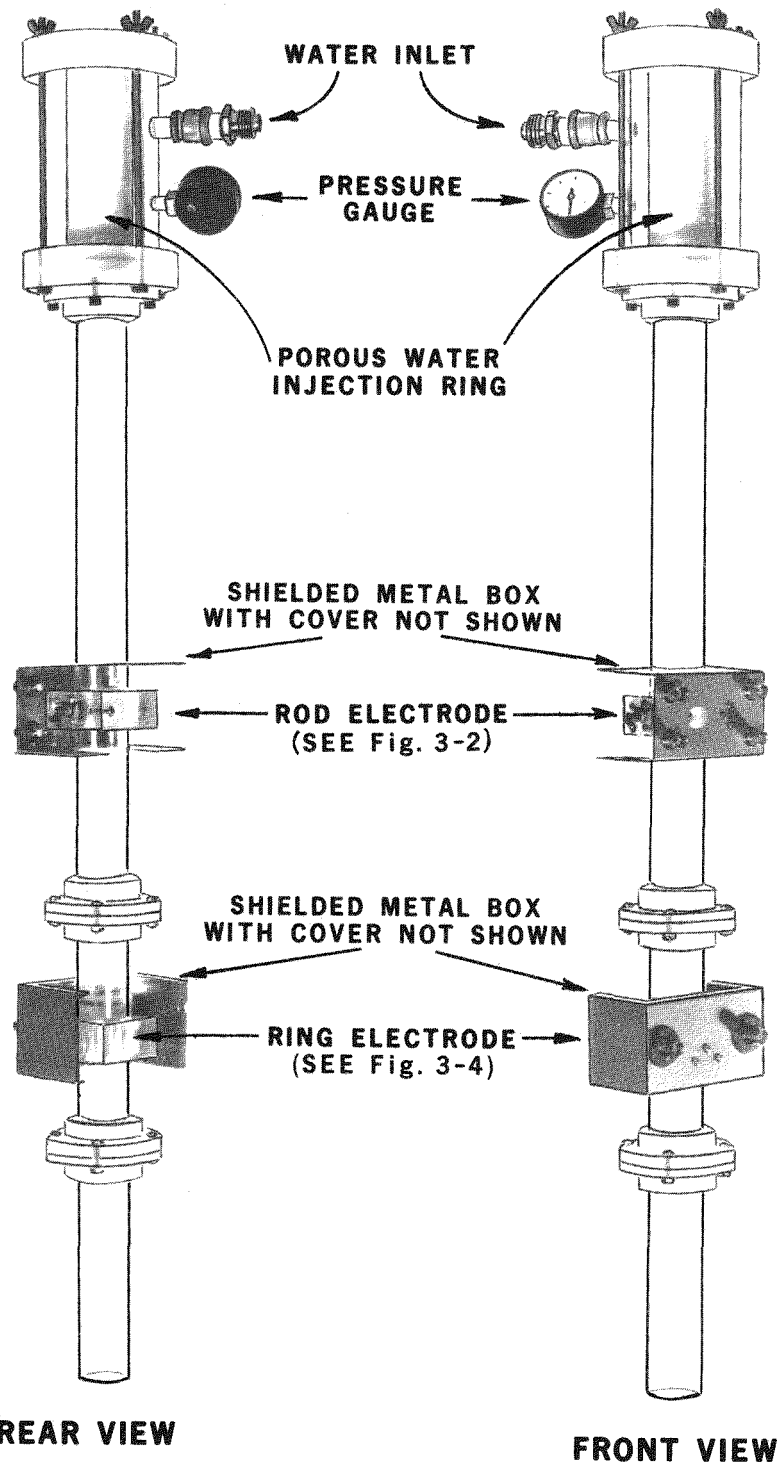


Figure 4-2. Assembly of the Dynamic Test Section

density and D is the tube diameter. At higher flow rates the film flow becomes turbulent and the thickness increases at a greater rate than the $1/3$ power predicted under laminar conditions. The onset of turbulence is governed by the film Reynold's number defined as

$$Re_T = \frac{4\rho_f Q_f}{\pi D \mu_f}$$

Normally the onset of turbulence is considered to occur for $Re_T > 2000$ but a reasonable fit to the entire flow region can be obtained if laminar flow conditions (δ proportional to $Q_f^{1/3}$) are assumed for $Re_T < 3000$ and turbulent flow conditions (δ proportional to $Q_f^{1/3}$) are assumed for $Re_T > 3000$.

If we insert the appropriate numbers for the pipe diameter and assume a water temperature of 17°C we find with Q_f expressed in gal/min and δ in cm.

$$\delta = 0.0593 Q_f^{1/3} \quad Q_f < 1.28 \text{ gal/min}$$

$$\delta = 0.0546 Q_f^{2/3} \quad Q_f > 1.28 \text{ gal/min}$$

This result is plotted in Fig. 4-3.

With this apparatus, film thicknesses ranging from less than 0.4 to 4 mm could be obtained with the existing water supply.

INSTRUMENTATION FOR CAPACITANCE MEASUREMENT

For the experimental investigation of water film thickness by means of capacitance methods, different types of instruments were considered. A Boonton 1 MHz Capacitance Bridge 76 A is capable of showing the values of capacitance, resistance, conductance, and Q factors. It has very good accuracy and very high resolution, but a slow response time, (about two measurements per second). This instrument is more suitable for the static calibration of the electrodes. In order to obtain similar accuracy and fast response, a capacitance meter from the same manufacturer Model No. 72BD, with a digital readout

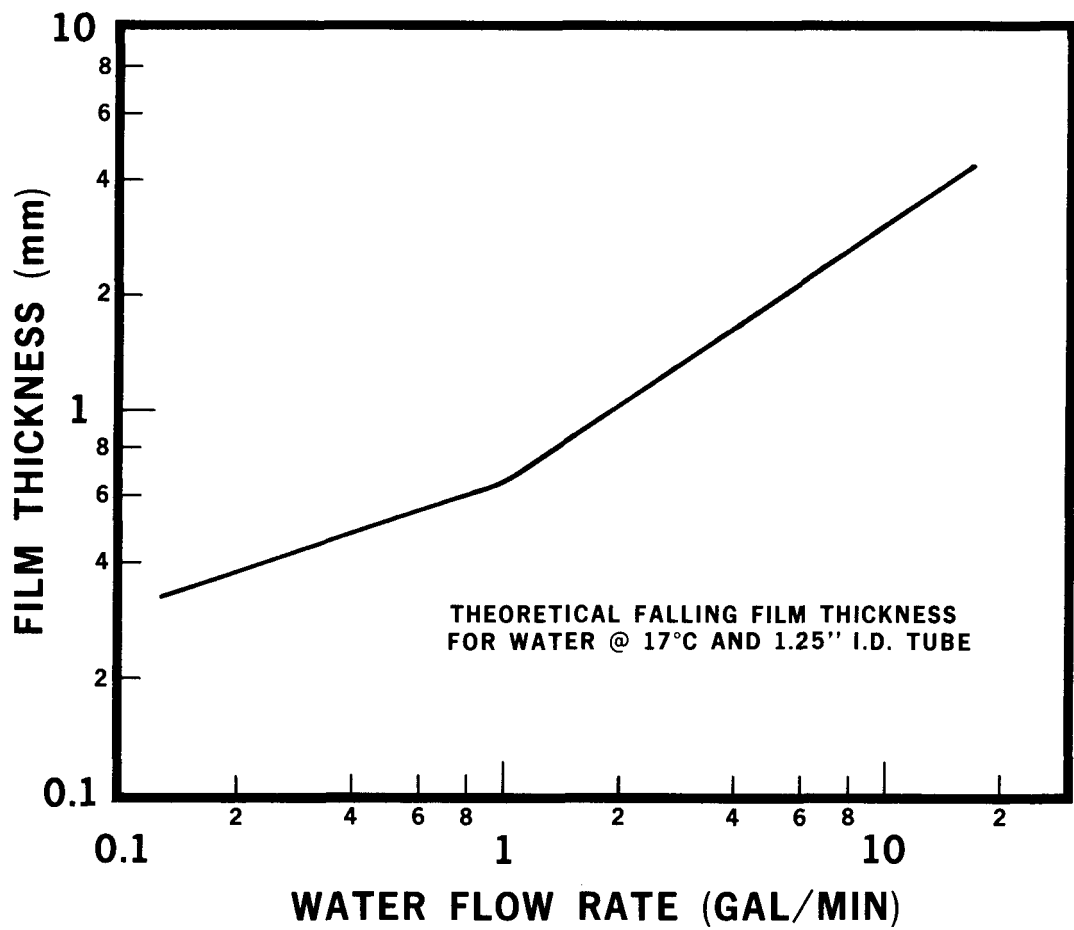


Figure 4-3. Water Film Thickness as a Function of Flow Rate

and a DC analog output was finally selected and was found to be satisfactory for both the static and the dynamic measurements. The meter has a cut-off frequency of about 600 Hz which is very important and useful for the dynamic detection of the water film waves generated during the annular flow. The analog output of the capacitance meter will provide a signal for visual observation or recording on a storage oscilloscope. The capacitance meter is sensitive enough to detect a capacitance change of .01 pF in 2 ms. The condition required for the capacitance meter 72BD to give an accurate readout is that a Q factor of a value better than 5. However, it had been tested and found that even with a Q as low as 0.9, the error in the result is still well within 1%. The requirement of a high Q however, is not a problem, as an external small capacitor can always be connected in parallel with the electrodes to increase the figure of merit. This can be verified by the experimental results obtained. The set up of equipment for static calibration is shown by a photo in Fig. 4-1. A storage oscilloscope, Tektronix 5113, with a model 5A22N Differential Amplifier and 5B92N Dual Time Base, was used for the measurement of the film thickness fluctuations.

Section 5

EXPERIMENTAL RESULTS

In this section experimental results are presented in order that a comparison can be made between the data obtained from the theoretical investigations and experimental observations and between the results of the static and dynamic calibrations. In addition, the influence of other parameters such as the conductivity of the water, the temperature of the fluid, and the Q factor are examined.

SELECTION OF ELECTRODE PATTERNS FOR THE ROD-TYPE ELECTRODE PAIR

In order to optimize the geometrical configuration of the rod-type electrodes, preliminary measurements were first made using electrodes of various shapes and sizes. To simplify the measurements, these electrodes were generated photographically on printed circuit boards. A number of samples are shown in Fig. 2-2. The initial capacitance of these kinds of electrodes is always very low because of the small thickness (0.016") of the copper sheet. In Fig. 3-1, two families of curves are shown to illustrate that the characteristics of the electrode pairs depends very much on their shape. Curves with a solid line (A, B, C, D, E) are taken from the electrode pairs with an outside diameter of 6 mm, while those with a dashed line (a, b, c, d, e) belong to the electrodes of 4.5 mm in outside diameter. The black line or curve within the circle, Fig. 3-1, represents the air-gap which is about 0.8 mm for the large electrodes and 0.6 mm for the small electrodes. From these curves, several conclusions can be drawn, namely, (1) the saturated capacitance increases with the size of the electrode by comparing families I and II, (2) the sensitivity of the electrode $\Delta C/\Delta t$, increases with the length of the gap, (by comparing A, B, C, etc) and (3) the dynamic range, i.e. the range of the water thickness from zero to the saturation value $\frac{\Delta C}{\Delta t} \approx 0$, increases with the transverse length of the gap, (comparing electrode E or e to the other electrodes in the same family).

The electrode C has a very simple geometric form, and in addition, has a relatively high sensitivity and a wide dynamic range. Based upon this preliminary investigation, it was thus decided to use pattern C with a diameter of 6 mm for the design of the rod electrode.

Pattern D is an electrode of coaxial form. It is a closed circuit with the least fringe effect, hence it is the most interesting electrode for comparison between the theoretical and experimental evaluations. This electrode system fits the theory quite well if the concentric gap is small compared to the width of the outer and inner electrodes. Since the inner electrode is a metallic disc, it reduces the fringing effect of the electrode to a great extent. An example is given in Fig. 5-1.

COMPARISONS BETWEEN STATIC AND DYNAMIC MEASUREMENTS

There were two kinds of rod electrodes tested; the ceramic electrode and the copper electrode. Since the data of the static measurements are taken by adding water to the container step by step, it is always possible to obtain a smooth curve with good consistency. In Fig. 5-2, two curves are shown which represent the measurement results for a ceramic electrode and a copper electrode. Obtained with low conductivity water, the curves differ from each other by about 20%, (less than 1 pf), which is understandable since the geometrical dimensions of the two electrodes are not exactly identical. The small triangle dots and crosses are the measured points from dynamic measurements taken at a different time. Misalignment of the rod electrode inside the tube will cause considerable deviation between the dynamic points and the static curve.

By accurate adjustment and the use of a rod electrode which has the probe end cut to the same curvature of the tube's inner wall so that it will be flush with the wall surface, the dynamic measured points fall on the static curve with good consistency (Table 5-1 & 5-2). The data was repeatable. This implies that static calibration is applicable to dynamic conditions. This fact is further strengthened by measurements of the ring electrodes. In Fig. 5-3 a curve is drawn through measured points represented by small circles taken with low-conductivity water, LCW, of conductivity $\delta = 6.67 \mu\text{S}/\text{cm}$, and by

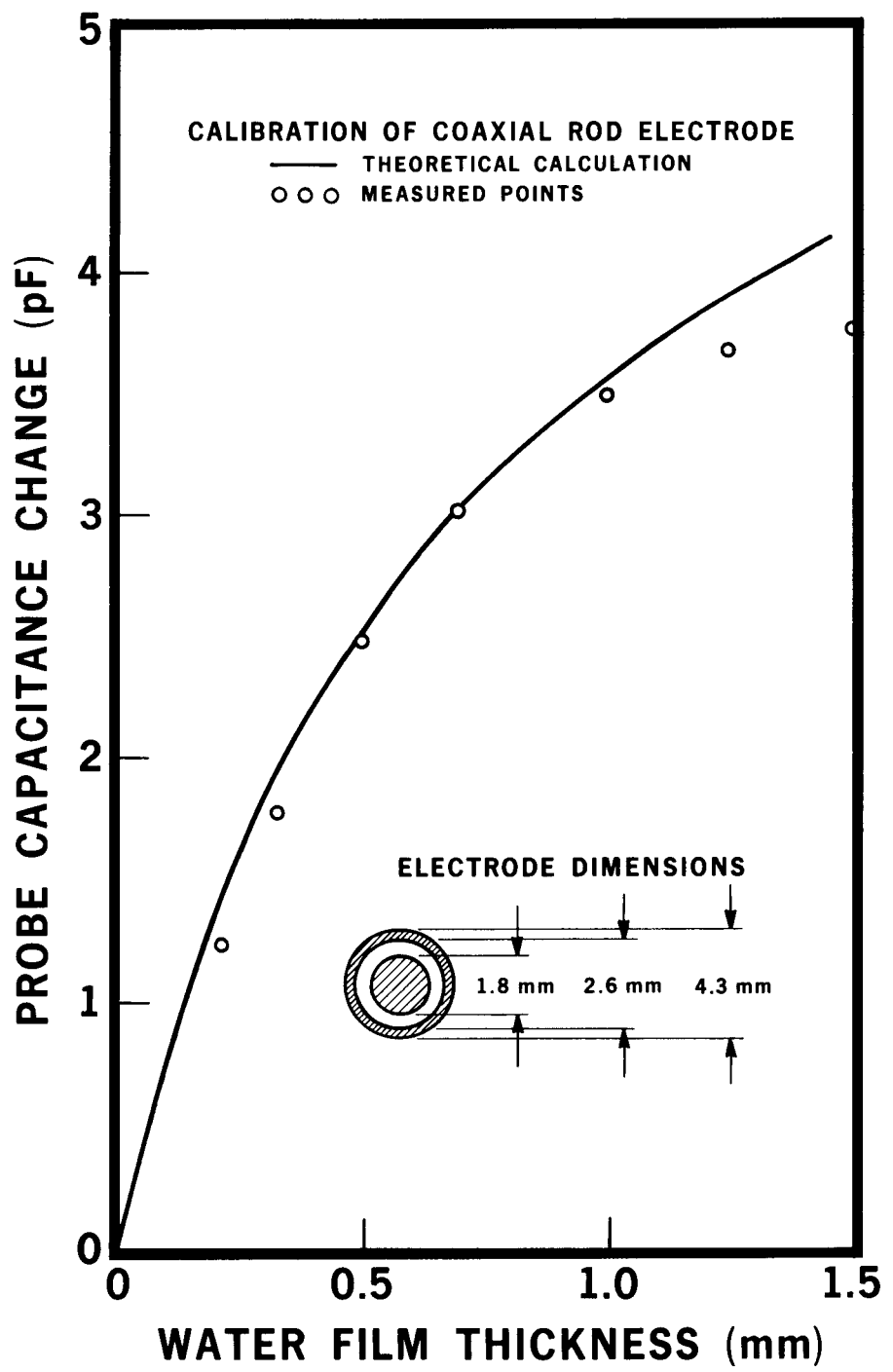


Figure 5-1. Comparison Between Theoretical and Measured Values of a Coaxial Electrode Pair

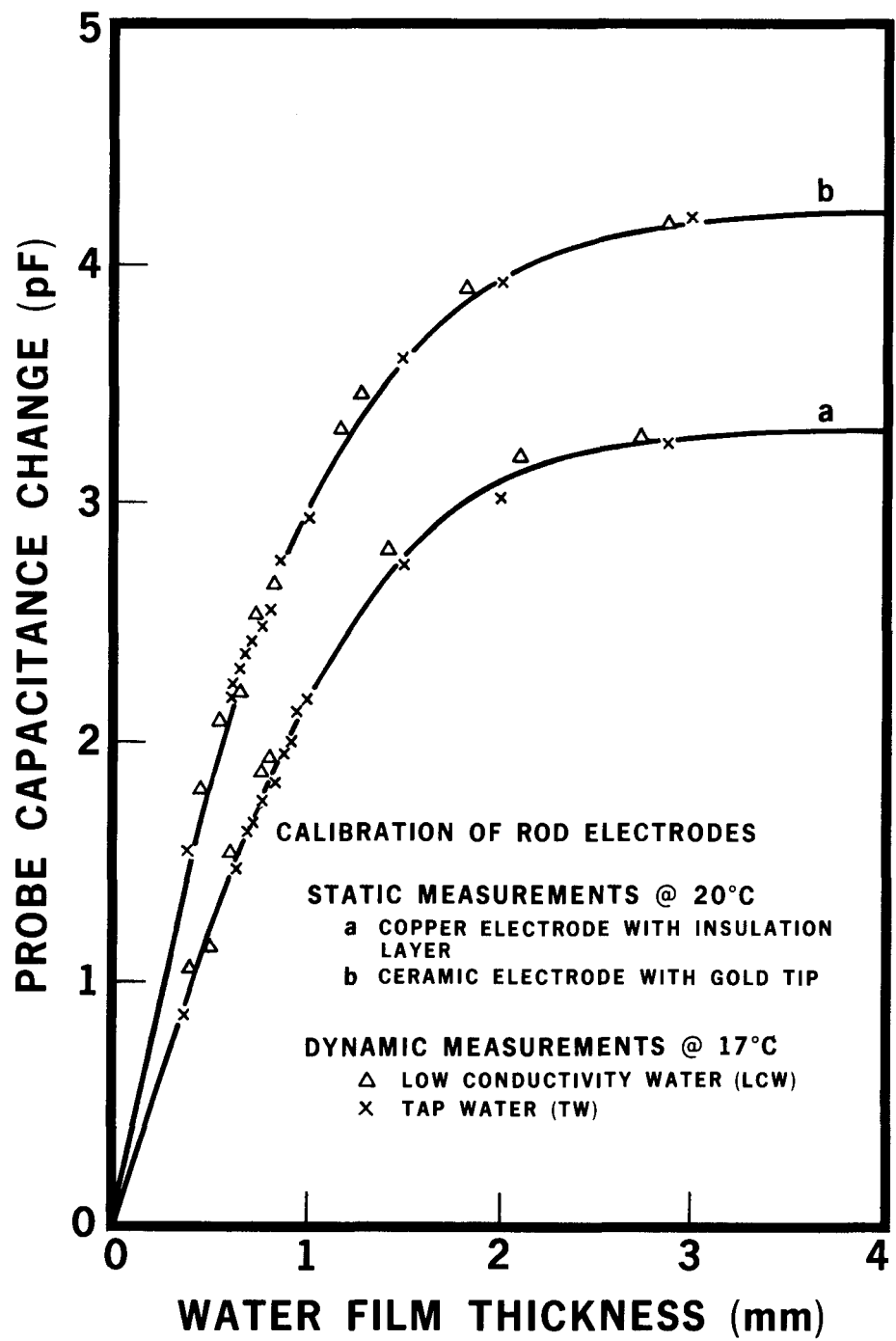


Figure 5-2. Experimental Results of Calibrations of Rod Electrodes (Static and Dynamic)

crosses taken with tap water, TW, of $\delta = 66.7 \mu\text{S}/\text{cm}$. There is practically no difference between LCW and TW in the experimental results from the static measurements, using two coplanar strips to represent the two ring electrodes.

The results of the dynamic measurements carried out on the ring electrodes are given in Fig. 5-4 where the large number of points were also taken at different times, with TW or LCW. The most significant and important fact is that all the points fall on the static curve with little deviation except those few points near 3 mm, which were at the time limited by the flow system. The ring electrode pair was mounted on the inner wall of the annular tube section and had the exact diameter as the tube. There was thus no problem of alignment, therefore the dynamic data coincided with the static curve as expected. In Tables 5-3 and 5-4 the experimental results are recorded.

INFLUENCE OF WATER TEMPERATURE AND CONDUCTIVITY ON FILM THICKNESS MEASUREMENT

The above experiments were carried out at room temperature. Since varying temperature may be present in the real system, it is important to determine the influence of temperature on the capacitance measurement. With regard to the electrode's own initial capacitance, it did not change value significantly when the electrodes were heated up by a hot air gun or cooled by a coolent spray. With a printed circuit electrode, it was noticed that with LCW (conductivity $\delta = 6.67 \mu\text{S}/\text{cm}$) the saturation capacitance changed by about 6% from 17°C to 49°C , while the capacitance within the dynamic range, i.e. below the knee of the saturation part of the curve, remained practically unchanged. When tap water ($\delta = 66.7 \mu\text{S}/\text{cm}$) was used, the temperature dependence was more pronounced. Within this temperature range, the variation of the measured saturation capacitance can be as high as 50%. The reason is that the conductivity of tap water available at LBL is high and it increases rapidly with temperature. The model 72BD Capacitance Meter requires a moderate quality factor, $Q = 5$, for reliable operation. For very small capacitance values, this restriction necessitates that the parallel leakage resistance be large (e.g. if $C = 1 \text{ pF}$ then $R \sim 1 \text{ M}\Omega$). The initial capacitance of the printed circuit electrodes were in general very low, less than 1 pF. The highly conductive tap water was not able to provide a sufficiently high resistive film above the electrode. To increase the Q factor, one can always connect an external, large capacitor parallel to the electrode (Fig. 5-5). This has been

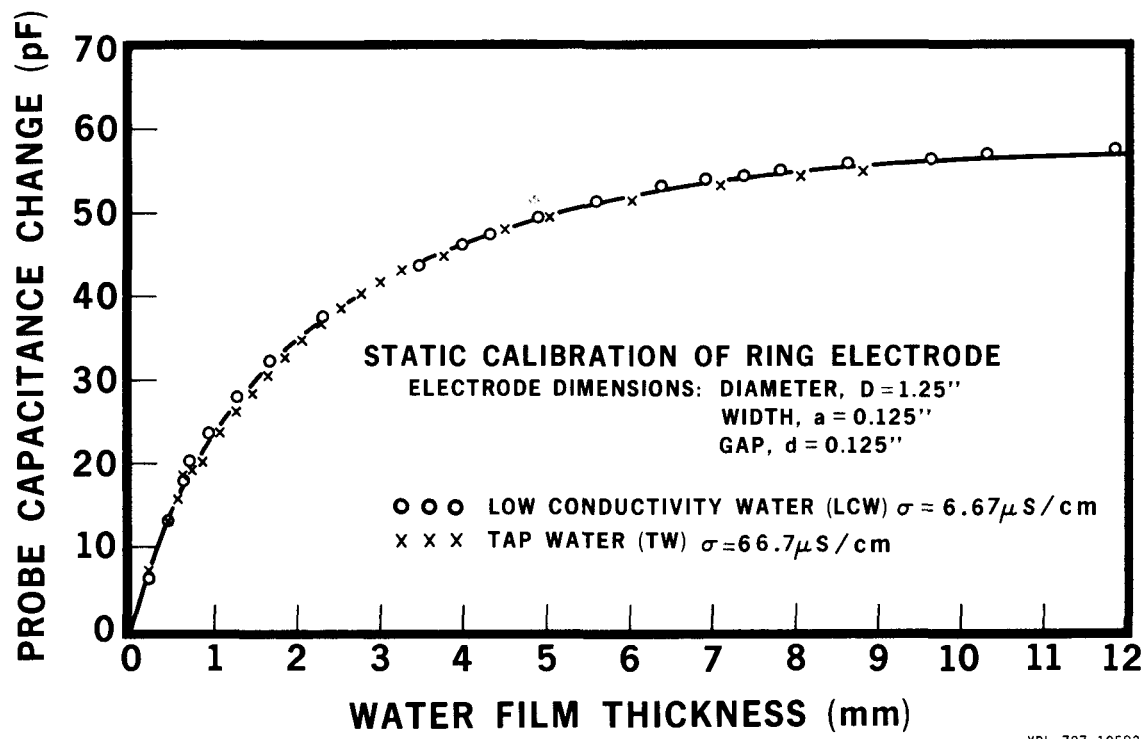


Figure 5-3. Static Calibration Curves of a Ring Electrode with LCW and TW

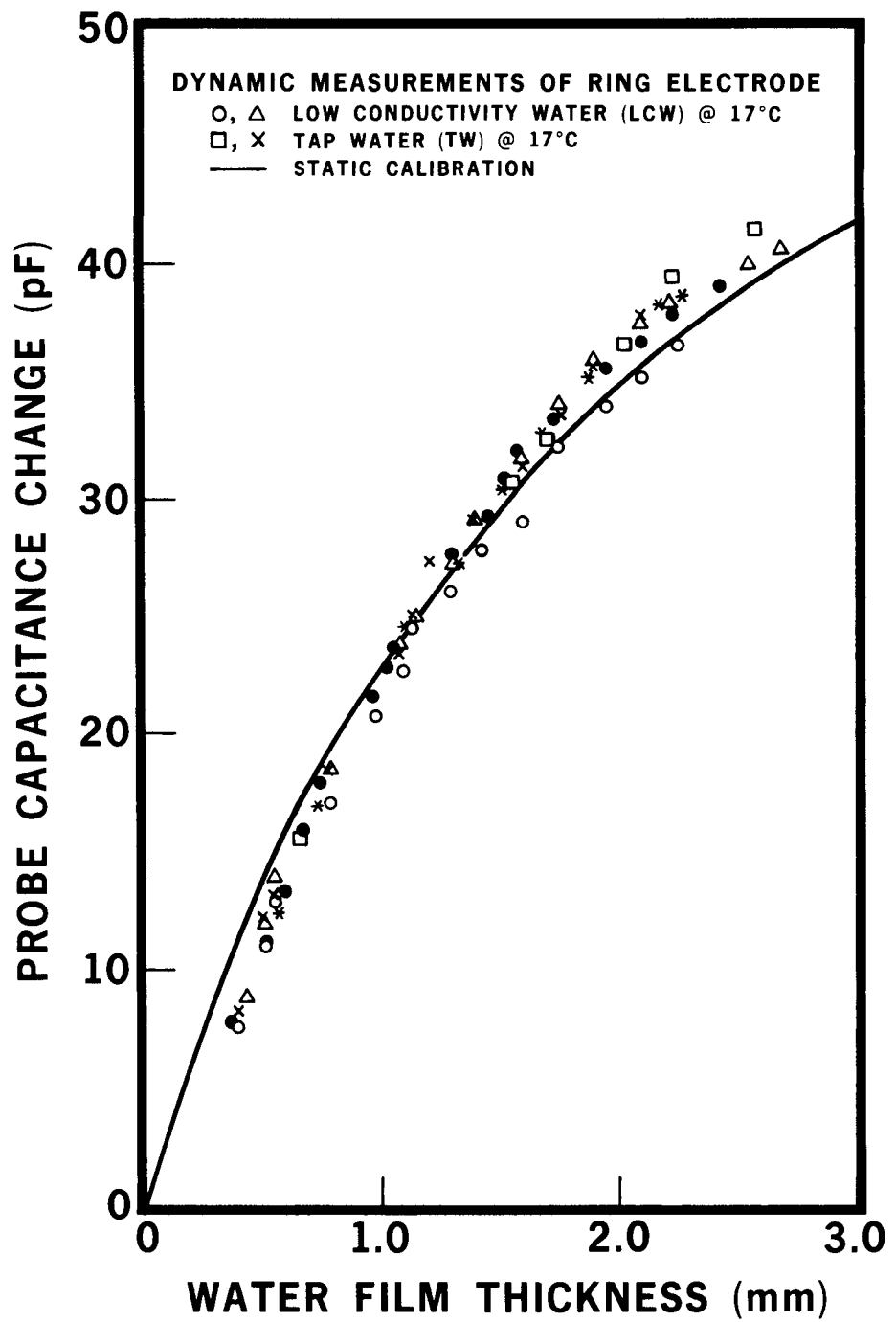


Figure 5-4. Dynamic Calibration of the Ring Electrode

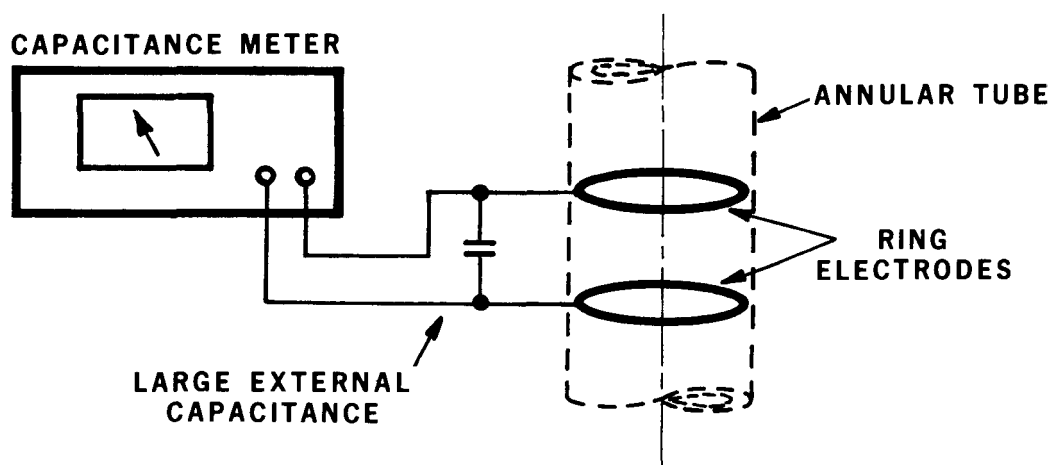


Figure 5-5. Arrangement of an External Capacitance for Improving Q Factor

tried and found to reduce the temperature dependence of the electrode capacitance to a large extent. The solid rod electrodes and the ring electrodes utilized for the experiment have comparatively large initial capacitances. The temperature effect was not observed, therefore, probably no significant temperature effects exist for the electrode of significant large capacitance. In theory, the capacitance itself depends only on the dielectric constant which is independent of temperature. If the conductivity of the flowing fluid should change according to the temperature and thus alter the value of Q to an unfavorable value, it is, as it has been pointed out, always possible to improve the Q factor by adding an external capacitor and restore the stability of the capacitance against temperature.

Table 5-1

STATIC MEASUREMENT OF ROD-TYPE ELECTRODES
WITH A 6 MM DIAMETER AND 0.8 MM INSULATION GAP

Water: Low Conductivity Water (LCW) at 20 C.

(I) Ceramic Electrode with Gold Tip
Initial $C_0 = 17.04 \text{ pF}$.

Film Thickness <u>t, mm</u>	Capacitance Increase <u>C, pF</u>
.245	.982
.398	1.580
.560	1.963
.778	2.525
1.002	2.970
1.244	3.340
1.588	3.675
1.911	3.909
2.608	4.390
3.010	4.180
3.313	4.204
3.744	4.210
4.123	4.202

Table 5-1 Continued

STATIC MEASUREMENTS OF ROD-ELECTRODES
WITH A 6 MM DIAMETER AND 0.8 MM INSULATION GAP

Water: Low Conductivity Water (LCW) at 20 C.

(II) Solid Copper Electrode
 $C_0 = 12.8 \text{ pF}$

<u>Film Thickness $t, \text{ mm}$</u>	<u>Capacitance Increase $C, \text{ pF}$</u>
.236	.621
.401	1.032
.617	1.437
.804	1.842
.970	2.139
1.270	2.522
1.578	2.862
1.994	3.084
2.270	3.175
2.555	3.222
3.906	3.301
4.272	3.298

Table 5-2
DYNAMIC MEASUREMENTS OF ROD ELECTRODES

Water: LCW at 18 C
(I) Ceramic Electrode With Gold Tip

1st Trial

Freq. <u>f, Hz</u>	Film Thickness <u>t, mm</u>	Capacitance <u>C, pF</u>
30	0.440	1.80
51	0.530	2.085
98	0.650	2.213
115	0.730	2.533
141	0.820	2.651
222	1.110	3.315
272	1.270	4.454
405	1.830	3.900
902	2.870	4.180

2nd Trial

27	0.442	1.380
64	0.560	1.644
121	0.720	2.040
136	0.800	2.307
295	1.375	3.280
662	2.322	3.950

3rd Trial

<u>Freq. f, Hz</u>	<u>Film Thickness t, mm</u>	<u>Capacitance C, pF</u>
20	0.38	1.542
78	0.60	2.187
80	0.61	2.235
86	0.622	2.281
90	0.630	2.314
105	0.675	2.375
112	0.710	2.420
125	0.760	2.484
238	0.811	2.555
142	0.830	2.756
211	1.080	2.935
322	1.400	3.602
540	2.040	3.930
950	2.980	4.182

Table 5-2 Continued
 DYNAMIC MEASUREMENTS OF ROD ELECTRODES

Water: LCW at 18 C
 (II) Solid Copper Electrode
 1st Trial

<u>Freq. f, Hz</u>	<u>Film Thickness t, mm</u>	<u>Capacitance C, pF</u>
22	.390	1.051
48	0.506	1.152
81	0.610	1.532
122	0.750	1.870
133	0.790	1.932
220	1.110	2.507
233	1.160	2.592
325	1.420	2.807
611	2.120	3.192
840	2.720	3.275

2nd Trial

13	0.33	0.860
46	0.50	1.198
90	0.63	1.470
106	0.68	1.618
115	0.722	1.652
132	0.787	1.754

<u>Freq. f, Hz</u>	<u>Film Thickness t, mm</u>	<u>Capacitance C, pF</u>
145	0.84	1.820
156	0.88	1.955
167	0.92	2.007
172	0.94	2.128
182	0.98	2.176
345	1.50	2.733
510	1.98	3.034
900	2.87	3.245

3rd Trial

20	0.38	1.542
78	0.60	2.187
80	0.61	2.235
86	0.622	2.281
90	0.630	2.314
105	0.675	2.375
112	0.710	2.420
125	0.760	2.484
238	0.811	2.555
142	0.830	2.756
211	1.080	2.935
322	1.400	3.602
540	2.040	3.930
950	2.980	4.182

Table 5-3
 STATIC MEASUREMENTS OF RING ELECTRODES USING STRIPS
 Width: 1/8", Gap = 1/8", Initial Capacitance Co: 2.6 pF
 (I) Water: LCW, 20 C

Film Thickness <u>t, mm</u>	Capacitance Increase <u>C, pF</u>
.205	6.52
.414	13.2
.735	20.8
.875	22.4
1.255	28.1
1.663	32.4
2.273	37.8
3.455	43.8
4.313	47.6
4.833	49.6
5.573	51.5
6.426	53.3
6.913	54.0
7.393	54.6
7.795	55.1
8.645	56.0
9.645	56.8
10.309	57.3

<u>Film Thickness t, mm</u>	<u>Capacitance Increase C, pF</u>
11.840	57.90
12.348	53.80
13.350	58.80
13.508	59.10
14.259	59.20

(II) TW, 20 C

0.215	7.10
0.455	13.10
0.577	15.80
0.674	17.90
0.768	19.30
0.872	20.40
1.080	23.60
1.275	26.00
1.466	28.40
1.654	30.60
1.873	32.60
2.081	34.50
2.332	36.60
2.584	38.60

<u>Film Thickness t, mm</u>	<u>Capacitance Increase C, pF</u>
3.017	41.80
3.520	44.10
3.740	46.40
4.404	48.10
5.075	49.00
5.556	50.60
6.033	51.40
7.075	53.20
8.040	54.25

Table 5-4
DYNAMIC MEASUREMENTS OF RING ELECTRODES

Diameter: 1 ", Width 1/8", Gap, 1/8"
Water: LCW & TW 17.7 C

(1) Water LCW*

Freq. of Water Gauge f, Hz	Film Thickness t, mm	Capacitance Increase C, pF
65	.57	12.4
116	.73	16.9
220	1.10	24.5
282	1.32	27.2
349	1.51	30.4
410	1.68	32.8
486	1.88	35.2
596	2.17	38.2
618	2.27	38.5

(1) Water LCW

24	0.4	8.8
57	0.51	11.9
78	0.55	13.9
132	0.79	18.5
210	1.08	23.9

Freq. of Water Gauge f, Hz	Film Thickness t, mm	Capacitance Increase C, pF
230	1.15	24.9
270	1.30	27.2
310	1.40	29.2
364	1.60	31.7
433	1.75	34.0
494	1.90	35.8
559	2.10	37.4
612	2.22	38.3
724	2.56	39.8
820	2.68	40.6

(1) Water LCW⁰

22	0.40	7.6
57	.51	11.0
78	.55	12.8
130	.79	17.0
160	.98	20.7
210	1.10	22.6
240	1.13	24.5
270	1.30	26.0
310	1.42	27.8
369	1.60	29.9

Freq. of Water Gauge f, Hz	Film Thickness t, mm	Capacitance Increase C, pF
432	1.75	32.1
499	1.95	33.9
560	2.10	25.2
620	2.25	26.5

(1) Water LCW[•]

19	.37	7.8
57	.51	11.6
76	.60	13.3
105	.67	15.9
132	.74	17.9
181	.97	21.6
192	1.02	22.8
206	1.07	23.6
279	13.00	27.6
325	14.50	29.2
354	15.20	30.8
364	15.80	32.0
432	17.30	33.4
433	17.30	33.5
505	19.50	35.5
563	21.00	36.7

<u>Freq. of Water Gauge f, Hz</u>	<u>Film Thickness t, mm</u>	<u>Capacitance Increase C, pF</u>
625	22.3	37.9
683	24.4	39.0

(2) Water TW

75	0.6	13.4
101	0.66	15.5
365	1.55	30.6
409	1.70	32.5
435	2.03	36.5
619	2.23	39.4
870	2.58	41.5

(2) Water TW^X

24	0.4	8.3
57	0.51	12.0
78	0.55	13.2
133	0.79	18.4
211	1.08	23.4
228	1.14	25.0
268	1.20	27.3
311	1.40	29.0

<u>Freq. of Water Gauge F, Hz</u>	<u>Film Thickness t, mm</u>	<u>Capacitance Increase C, pF</u>
370	1.60	31.4
435	1.76	33.6
495	1.90	35.6
557	2.10	37.8
613	2.22	38.5

Section 6

DISCUSSIONS AND CONCLUSIONS

We have investigated, experimentally and theoretically, two types of capacitance probes for making water film thickness measurements in annular two-phase flow configurations.

Capacitance probes of the rod-type are useful for making local measurements. However, as we have seen, their dynamic range is limited. For the probes considered in this report, the maximum film thickness which can be reliably measured is approximately 1-2 mm. The only way that the film thickness range can be increased is to enlarge the physical size of the probes. Thus, localization and thickness range are competing constraints subject to compromise. The rod-type electrodes have the advantage that they can be easily installed in the flow tube at any desired position.

The ring-type electrodes, on the other hand, have superior sensitivity and dynamic range. As shown above, they have the capability of making film thickness measurements up to 4-5 mm. Because they completely encircle the flow tube, measurements with these probes are averaged over a larger area. The ring-type probes are more difficult to construct and cannot be repositioned as easily as the rod electrodes.

As can be seen from the calibration curves (for example Fig. 5-2 and Fig. 5-3), the response of both types of probes to changing film thickness is non-linear. It is necessary to provide a linearizing transformation to the capacitance measurement to obtain the proper film thickness. This linearization can be accomplished either digitally by a data analysis system, or in an analog fashion by appropriate electronic circuitry. An analog linearizer, which would provide an immediate conversion, is presently under consideration. Because of the rapid response capabilities of the model 72BD capacitance

meter, it is possible to detect the fluctuations and wave motions of the water film passing over the capacitance probes. The oscilloscope photographs shown in Fig. 6-1 and 6-2 illustrate the variations in measured capacitance for each type of probe caused by fluctuations in the film thickness. In the photographs the amplitude of capacitance fluctuations is shown together with the mean capacitance value and the calculated average film thickness as determined by measuring the total water flow rate. The fluctuations are due to turbulences in the film flow which occur for film Reynold's numbers in excess of about 2000 as described above.

In order to determine the thickness fluctuations of the film from the photographs, it is necessary to apply the linearizing transformation derived from the calibration curves. For example, in Fig. 6-1d, the mean film thickness is 3.0 mm which for the ring-type electrodes is well within the dynamic range of the probe. The film thickness fluctuations can be obtained from the capacitance fluctuations of approximately 3.5 pF and the slope of the transfer curve yielding 3 ± 0.35 mm for this case. On the other hand, the data in Fig. 6-2d obtained with the rod-type electrodes and a mean film thickness of 3mm, shows a small capacitance fluctuation. This is because the probe is almost saturated. Even with a linearizing circuit, one would not expect to obtain reliable information in this case.

We have evaluated the capacitance methods as a technique for making film thickness measurements in two phase flow systems. Two types of probes have been designed; rod-type electrodes and ring-type electrodes. The former type permits the measurement of localized film thicknesses within their dynamic range of 1-2 mm and the latter type enables us to measure cylindrically averaged thicknesses with greater precision and with a dynamic range in excess of 5 mm. With calibration and appropriate linearization, the capacitance measurements can be made to yield thickness data directly and with rapid time response. The latter capability makes it possible to observe fluctuations and wave motions in the film flow provided they are within the dynamic range of the probe used. Finally, we point out that the probes are non-intrusive and do not require doping or other modification of the water supply.

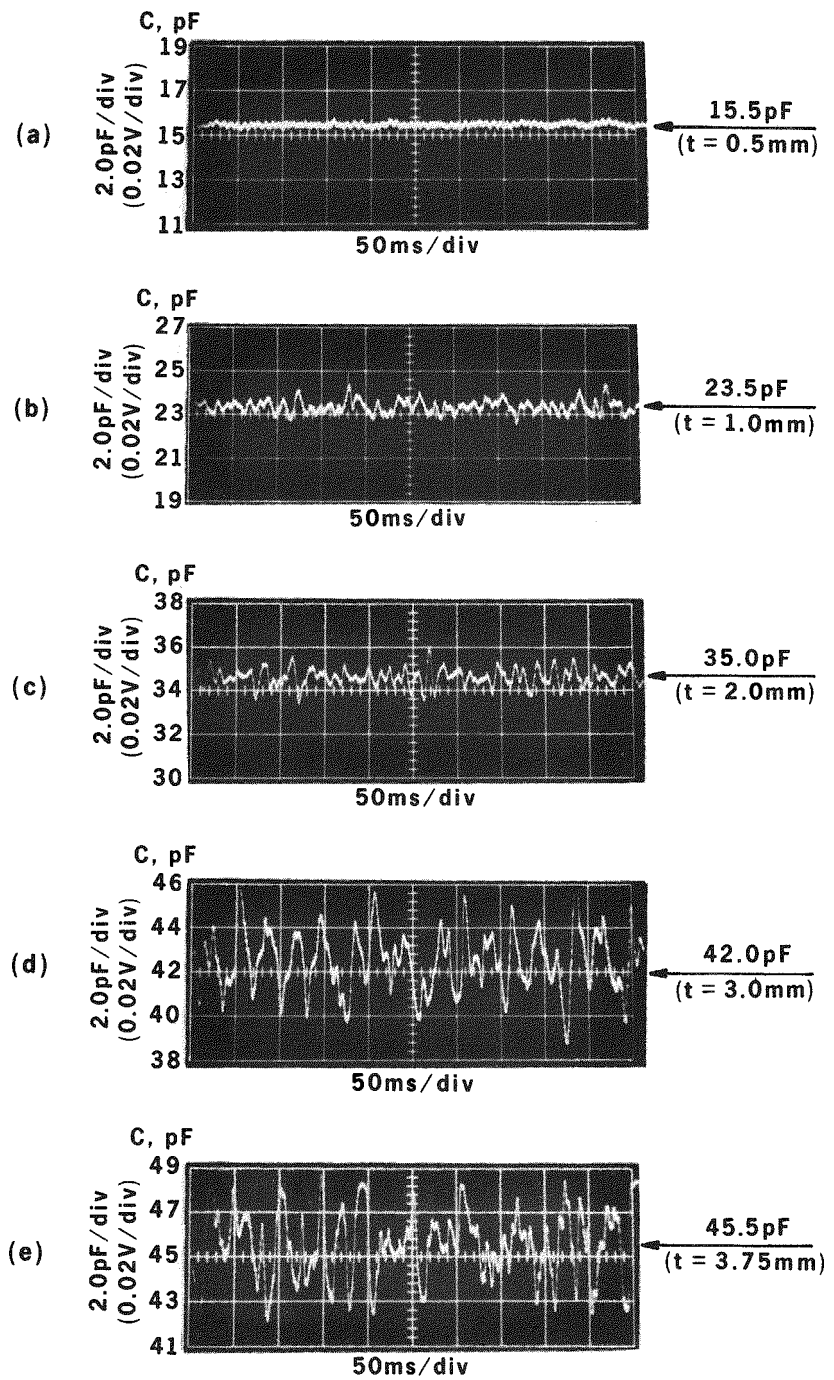


Figure 6-1. Transient Measurements of Film Thickness with Ring Electrodes

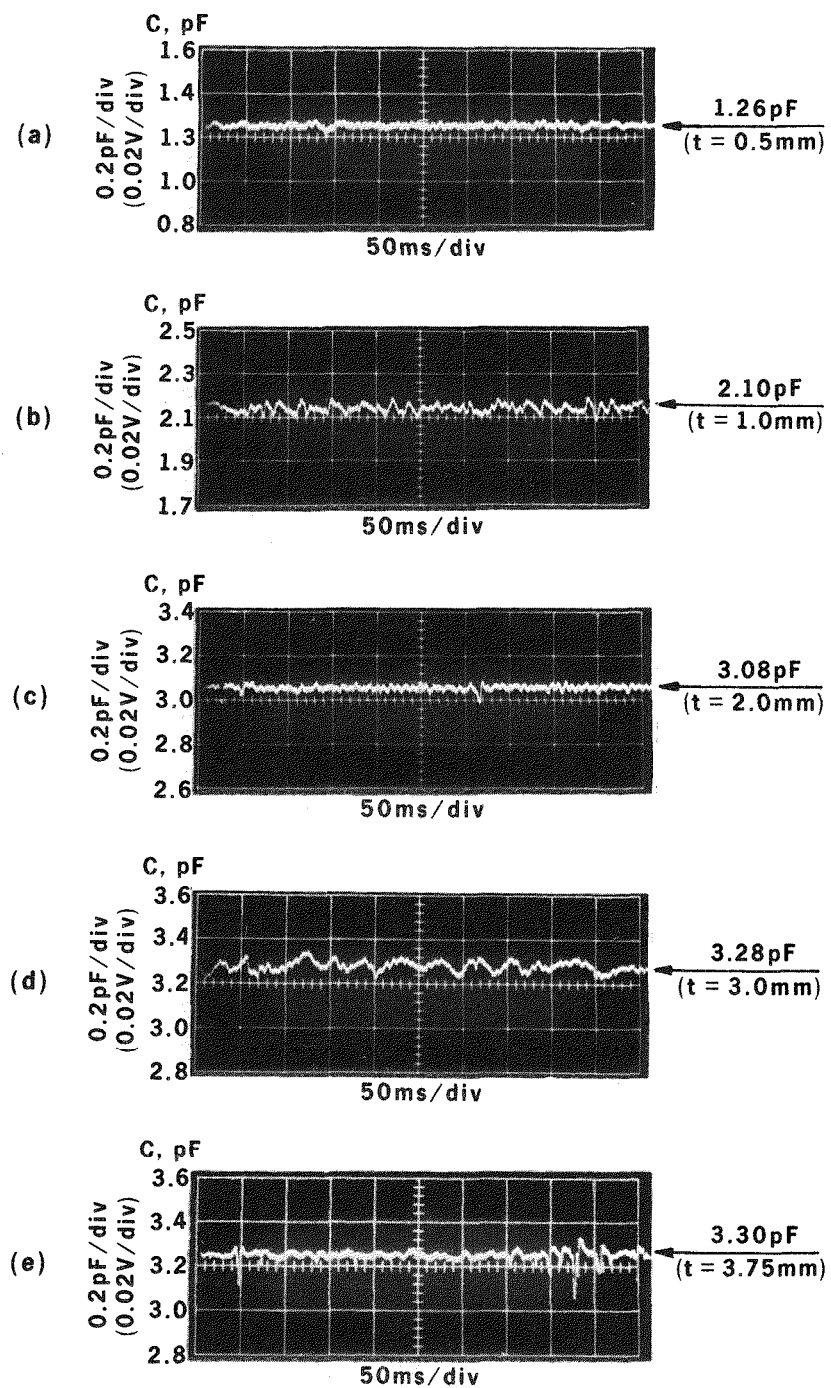


Figure 6-2. Transient Measurements of Film Thickness with Rod Electrodes

Appendix A
DERIVATION OF EQUATION 2-1

In Fig. A-1b we show a cross sectional view of a pair of coplanar capacitance electrodes covered with a water film thickness, t . In order to carry out the calculation, we consider a pair of infinite parallel plates in the W -plane, Fig. A-1a, in which the lines of flux function V perpendicular to the lines of potential function U , is transformed to a pair of coplanar electrodes in the Z plane, having their width and spacing along the X -axis, and the fluid film thickness, t along the Y -axis. By means of the Schwarz-Christoffel transformation (16), we have:

$$Z = \operatorname{Sin} W \quad (A-1)$$

where $Z = X + jY$ and $W = U + jV$, and it follows that:

$$\frac{X^2}{\operatorname{Cosh}^2 V} + \frac{Y^2}{\operatorname{Sinh}^2 V} = 1 \quad (A-2)$$

$$\frac{X^2}{\operatorname{Sin}^2 V} - \frac{Y^2}{\operatorname{Cos}^2 U} = 1 \quad (A-3)$$

and

$$X = \operatorname{Sin} U \operatorname{Cosh} V, \quad (A-4)$$

$$Y = \operatorname{Cos} U \operatorname{Sinh} V. \quad (A-5)$$

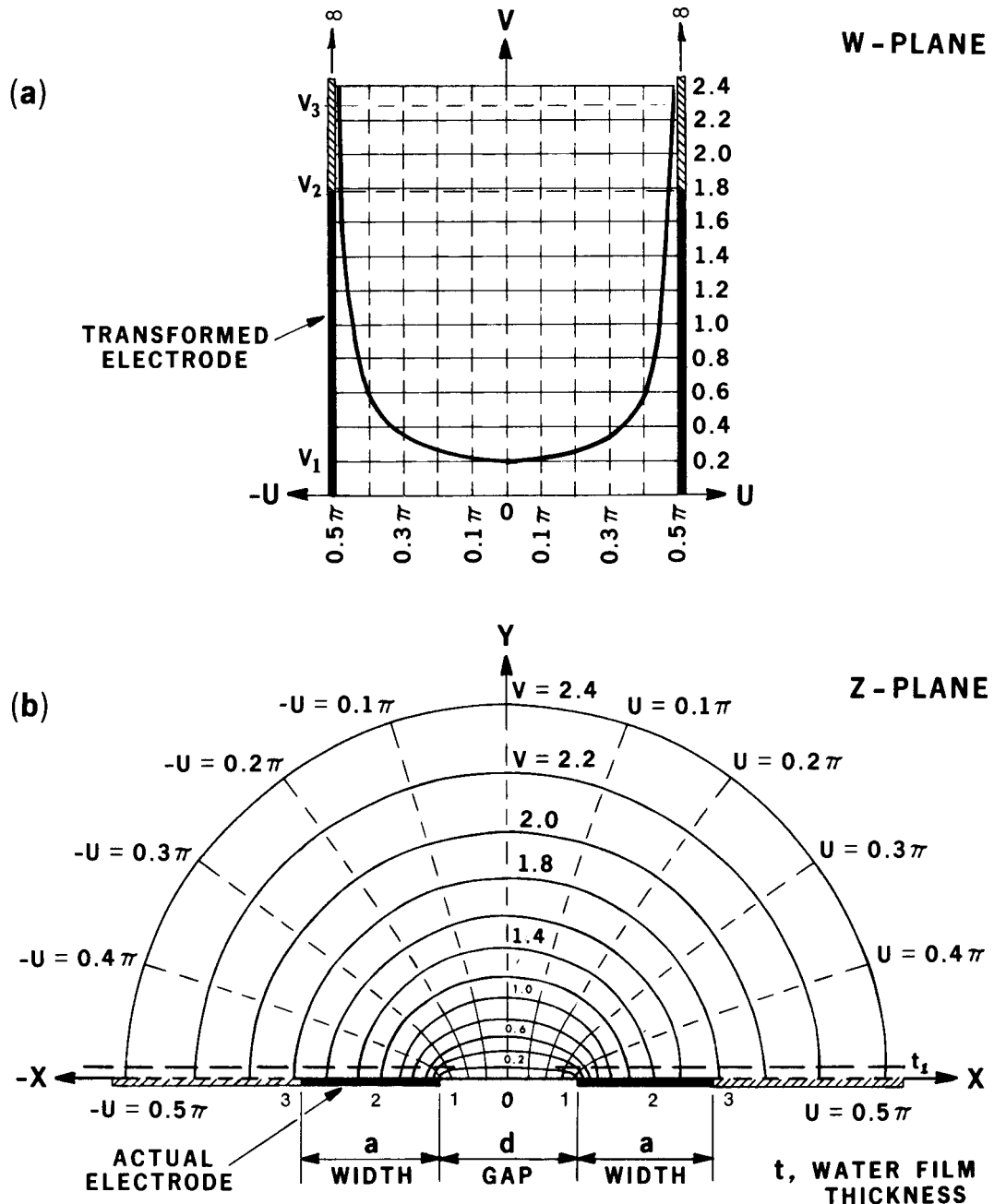


Figure A-1. Simple Conformal Transformation of Coplanar Electrode Pair (Hyperbolic Function)

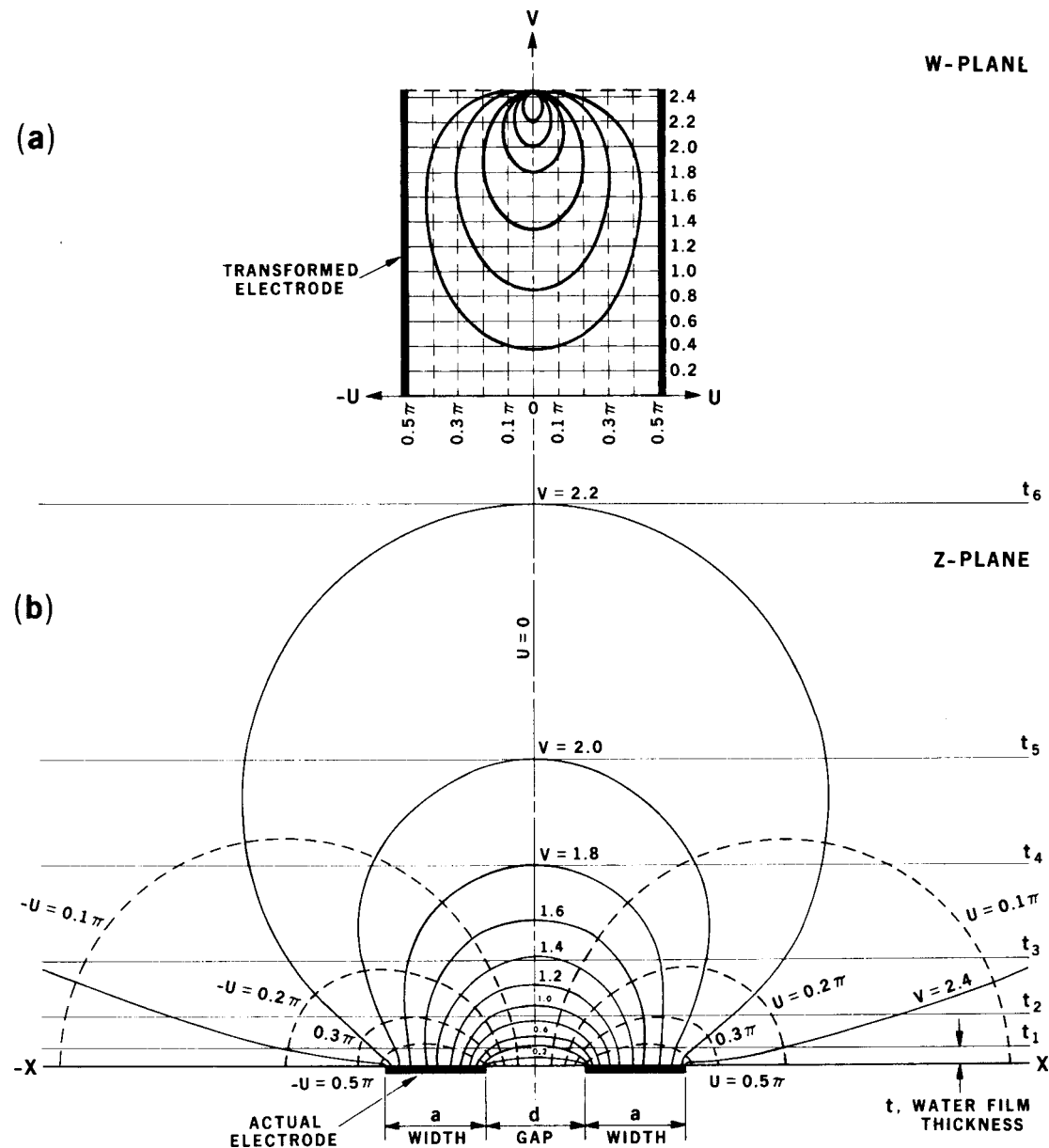


Figure A-2. Field Plotting of Coplanar Electrode Pair with Transformation $Z = SnW$ (Elliptical Function)

The curves in the Z-plane show a set of confocal ellipses for V equal to a constant and a set of confocal hyperbolas for U equal to constants. A fluid film of thickness t on top of the electrodes in the Z-plane will have a parabolic shape between the parallel electrodes in the W-plane. This configuration is utilized for the calculation of the capacitance.

The field plots in Fig. A-1 assume that the electrode pair has a width approaching infinity. If the electrode pair has a finite width, the field distribution is altered at the edges of the electrode yielding a pattern as shown in Fig. A-2, which is obtained from the conformal transformation with $Z = \text{Sn } W$ (17, 18), where $\text{Sn } W$ is the complex elliptical sine. A fluid film of thicknesses t_1, t_2, t_3, t_4 , and t_5 , on top of the electrodes in the Z-plane will appear as ellipses in the W-plane. When this pattern is used for the calculation of the capacitance, the equation is complicated by terms containing elliptical function and is difficult to solve.

The pattern in Fig. A-1 is more tractable, because it can be solved in terms of hyperbolic functions which are more easily evaluated. The fringe effect of the parallel electrodes with a finite width in the W-plane can be taken care of by increasing the width V_2 (corresponding to "a" in Z-plane) to an effective length V_3 , within which the field distribution is now considered to be uniform, and by the inclusion of a factor A, defined below, account for the saturation of the capacitance.

Suppose a pair of parallel plate electrodes having a width W and an insulated gap D . The gap space is filled with two insulating materials of dielectric constants k_1 and k_2 , respectively. The material of k_1 occupies the middle of the gap and has a thickness of B (Fig. A-3).

The capacitance c per unit length ℓ of this pair of electrodes will be obtained as:

$$\frac{c}{\ell} = \frac{k_2 \epsilon_0 W}{D \left[1 + \frac{B}{D} \left(\frac{k_2}{k_1} - 1 \right) \right]} \quad (\text{A-6})$$

where ϵ_0 = permittivity of vacuum.

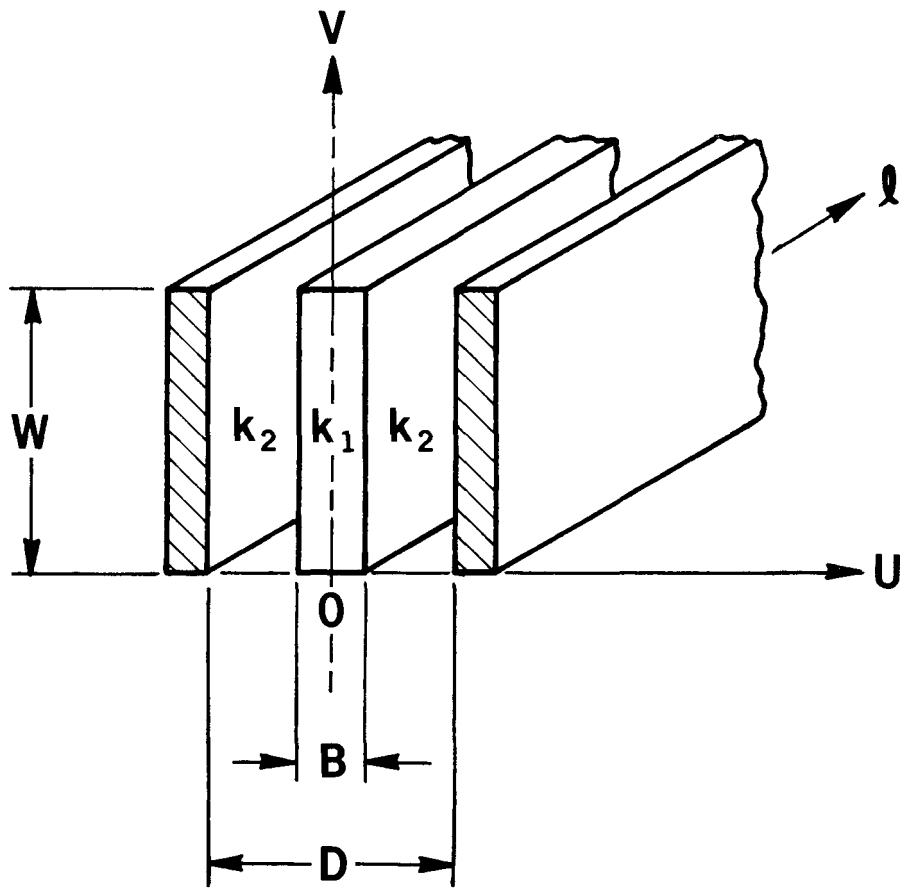


Figure A-3. Parallel Electrode Geometry with Two Dielectric Substances in Gap

The capacitance of the electrode pair shown in Fig. A-1a can thus be calculated with the following substitutions: $k_1 = 1$ (for air), $k_2 = 80$ (for water), $W = dV$, $D = \pi$, and $B = 2U$, namely,

$$\frac{C}{\lambda} = \frac{k_2 \epsilon_0}{\pi} \int f(U, V) dV \quad (A-7)$$

Since $U = \cos^{-1} \frac{Y}{\sinh V}$ (see eq. A-5), we have, for the given water thickness t_1 in Z-plane with the dimension normalized to the gap length $d = 2$

$$U = \cos^{-1} \frac{\frac{t_1}{d/2}}{\sinh V} \quad \text{in radians} \quad (A-8)$$

In terms of V , the normalized thickness $(\frac{t_1}{d/2})$ is expressed as:

$$\frac{t_1}{d/2} = \sinh V_1 \quad (A-9)$$

where V_1 is the point at the V axis of the W plane Fig. A-1.

The outside edge of the coplanar electrode (at the point $a + \frac{d}{2}$) in Z-plane is transformed to

$$V_2 = \cosh^{-1} \left(1 + 2 \frac{a}{d} \right) \quad (A-10)$$

Before the integration can be carried out to evaluate the total capacitance, the fringe effect of the electrode should be considered. Because of the finite width of the electrode, the field distribution at the edge will not be uniform, an effective length of $\frac{\pi}{8}$, will be added to V_2 so that the field distribution may be considered as uniform, and the integration should be carried on to its limit V_3 which is:

$$V_3 = V_2 + \frac{\pi}{8} \quad (A-11)$$

hence, we have

$$\begin{aligned}
 \frac{c}{\ell} &= \frac{k_2 \epsilon_0}{\pi} \int_{V_0}^{V_3} f(U, V) dV \\
 &= \frac{k_2 \epsilon_0}{\pi} \left[\int_0^{V_1} dV + \int_{V_1}^{V_3} \frac{dV}{1 + \frac{2(k_2 - 1)}{\pi} \cos^{-1} \frac{\sinh V_1}{\sinh V}} \right]
 \end{aligned} \tag{A-12}$$

This equation does not show the saturation effect with the water thickness increasing beyond the effective length V_3 . This can be taken care of with the introduction of a correction factor A , which implies that: (1) if the water level is less than V_2 , no correction is necessary, i.e. $A = 0$, and the integration is carried out simply for $V = 0$ to $V = V_3$ or

$$\frac{c}{\ell} = \frac{k_2 \epsilon_0}{\pi} \left[\int_0^{V_3} dV + \int_{V_1}^{V_3} \frac{dV}{1 + \frac{2(k_2 - 1)}{\pi} \cos^{-1} \left(\frac{\sinh V_1}{\sinh V} \right)} \right] \tag{A-13}$$

for $V_1 < V_2$; (2) if the water level is larger than V_2 and less than V_3 , a correction factor should be applied to the region between V_2 and V_3 to reduce the capacitance exponentially, so that it diminishes in the neighborhood beyond V_3 . This factor is given as

$$A = \exp \left[-\frac{8}{\pi} (V_1 - V_2) \right] \tag{A-14}$$

and the integration is obtained as

$$\begin{aligned}
 \frac{c}{\ell} &= \frac{k_2 \epsilon_0}{\pi} \left[\int_0^{V_2} dV + \int_{V_2}^{V_1} (1 - A) dV \right. \\
 &\quad \left. + \int_{V_1}^{V_3} \frac{(1 - A) dV}{1 + \frac{2(k_2 - 1)}{\pi} \cos^{-1} \left(\frac{\sinh V_1}{\sinh V} \right)} \right]
 \end{aligned}$$

$$\begin{aligned}
&= \frac{k_2 \epsilon_0}{\pi} \int_0^{V_1} dV + \int_{V_1}^{V_3} \frac{dV}{1 + \frac{2(k_2 - 1)}{\pi} \cos^{-1} \left(\frac{\sinh V_1}{\sinh V} \right)} \\
&- \int_{V_2}^{V_3} \frac{AdV}{1 + \frac{2(k_2 - 1)}{\pi} \cos^{-1} \left(\frac{\sinh V_1}{\sinh V} \right)} \quad (A-15)
\end{aligned}$$

for $V_2 < V_1 < V_3$ and (3) if the water level is larger than V_3 , the correction factor remains the same, the equation of capacitance is modified to:

$$\frac{C}{\lambda} = \frac{k_2 \epsilon_0}{\pi} \left[\int_0^{V_3} dV - \int_{V_2}^{V_3} \frac{AdV}{1 + \frac{2(k_2 - 1)}{\pi} \cos^{-1} \left(\frac{\sinh V_1}{\sinh V} \right)} \right] \quad (A-16)$$

for $V_2 < V_3 < V_1$.

The case (2) is applicable to our measurements and is given in the text as Eq. 2-1.

REFERENCES

1. D. Thornton and J. A. R. Bennet,, Transactions of the Institute of Chemical Engineering Vol. 39, 1961 , p.101.
2. G. F. Hewitt, R. D. King and P. C. Lovergrove, Chemical and Process Engineering , April 1964, p. 200.
3. J. G. Collier and G. F. Hewitt, "Film Thickness Measurements" AERE-R4684, 1964.
4. A. E. Dukler and D. P. Bergelin, Chemical and Process Engineering Vol. 48, 1952, p. 557.
5. S. R. Tailby et al. Transactions of the Institute of Chemical Engineering, Vol. 38, 1960.
6. M. R. Ozgu and J. C. Chen, "A Capacitance Method for Measurement of Film Thickness in Two-Phase Flow". Review of Scientific Instruments, Vol. 44, No. 12, Dec. 1973.
7. J. C. Chen et al. "Two-Phase Flow Instrumentation Research." Presented at the 5th Water Reactor Safety Research Information Meeting, November 7-11, 1977.
8. R. K. Sundaram, E. J. London, and J. C. Chen, "Development of Instrumentation for the Measurement of Thickness and Velocities of Thin Water Films" Presented at the 6th Water Reactor Safety Research Information. Washington, D. C., November 6-9, 1978.
9. R. Ozgu and J. C Chen, "Local Film Thickness During Transient Voiding of a Liquid Filled Channel". Presented at the Winter Annual Meeting of the American Society of Mechanical Engineers, Houston, Texas, November 30, 1975.
10. N. Hall-Taylor, G. F. Hewitt and P. M. C. Lacey, "The Motion and Frequency of Large Disturbance Waves in the Annular Two-Phase Flow of Air-Water Mixture". Chemical Engineering Science, Vol. 18, 1963, p. 537-552.
11. K. J. Chu and A. C. Dukler "Statistical Characteristics of Thin, Wavy Film, AIChE Journal. Vol. 21, No. 3, May 1975, p. 588-593. Also in IEChE Journal Vol. 20, No. 4, July 1974 p. 695-706.
12. A. E. Dukler "Characterization Effects and Modeling of the Wavy Gas-Liquid Interface," Progress in Heat and Mass Transfer Vol. 6, 1972, p. 207-234.

13. R. S. L. Lee and David: "A Study of Droplet Hydrodynamics Important in Local Reflood," Quarterly Progress Report, January 1-March 21, 1978, College of Engineering and Applied Science, State Univ. of N. Y., at Stony Brook.
14. R. T. Lahey, Jr. G. Krycole. "Two-Phase Flow Instrumentation Research at RPI". Rensselaer Polytech. Institute, Troy, New York, 1978.
15. Two-Phase Flow Instrumentation Review Group Meeting. Proceedings of the Meeting, January 13-14, 1977. Office of Nucl. Regulatory Research U. S. Nucl. Regulatory Commission.
16. H. Kober, Dictionary of Conformal Representations, New York, Dover Publications Inc. 1957.
17. Smythe, Static and Dynamic Electricity, New York, McGraw-Hill (1968).
18. N. B. Morton, Philosophy Magazine Vol. 2, p. 827, 1926.
19. G. B. Wallis, One Dimensional Two-Phase Flow, MaGraw-Hill Book Co., New York, (1969).